

**Assessment of station metadata in Alaska based on
analysis of Love waves from the 2012-04-11 M_w 8.6
offshore Sumatra earthquake, Version 5 (January 27, 2014)**

Carl Tape

carltape@gi.alaska.edu

Geophysical Institute, University of Alaska Fairbanks

Waveforms and metadata extracted: January 21, 2014

Previous versions of this report:

Version 4: June 13, 2013 (waveforms and metadata extracted on June 13, 2013)

Version 3: November 19, 2012 (waveforms and metadata extracted on November 17, 2012)

Version 2: August 16, 2012 (waveforms and metadata extracted on August 7, 2012)

Version 1: July 5, 2012 (waveforms and metadata extracted on April 28, 2012)

Technical Report
Alaska Earthquake Center
2012

Published online: January 27, 2014

Contents

1	Stations not in operation	3
2	Selection and processing of seismograms	4
3	Thresholding stations for scientific analysis	4
3.1	115 to 113: Eliminating (2) records without three components	4
3.2	113 to 104: Eliminating (9) records with data gaps	5
3.3	104 to 100: Eliminating (4) “odd-looking records”	5
3.4	100 to 93: Eliminating (7) records based on suspected instrument response errors (amplitude or phase)	5
3.5	93 to 86: Eliminating (7) HH records based on gaps or other problems	6
3.6	Other problematic records that should probably be cut	6
4	Station misalignments	7
5	Results by network	8
6	Recommendations for networks in Alaska and for the AEC database of waveforms and metadata	9
	References	11

Overview

This report is part of a detailed investigation of a M_w 3.9 earthquake near Nenana, Alaska, that was triggered by Love waves from a M_w 8.6 offshore Sumatra earthquake. Results from that study appeared in *Tape et al.* (2013). We analyze all BH and HH channel waveforms that are available at the Alaska Earthquake Center.

This report has three objectives:

1. to provide information that may help improve station metadata at Alaska stations
2. to provide a snapshot of station performance in Alaska at one particular time (11-April-2012)
3. to provide details and figures on part of the waveform processing used in *Tape et al.* (2013) (see report version 3)

This is the fifth version of this report. It should be continually updated, as long as updates for station metadata (on the epoch containing 11-April-2012) are made, since the changing metadata will influence our scientific analysis (e.g., Table 9). See below for a summary of previous versions of the report.

Please contact Carl Tape (carltape@gi.alaska.edu) if you have suggestions for improving the information in these notes. The hope is to establish this kind of analysis in an automated fashion, so that we can routinely assess station performance using a variety of relatively simple data processing tools.

IMPORTANT NOTES:

1. All waveforms were obtained from AEC, not IRIS. In several cases for non-AK stations, I have checked that the IRIS waveforms match those used in this analysis. In other cases, like some CN stations (Figure 7), the waveforms are not available at IRIS. Waveforms represent the network codes listed in Table 1.
2. All station metadata were obtained from AEC, not IRIS. However, the metadata should be the same. For networks AK (including the former XZ stations) and PS, AEC is responsible for metadata. For all other networks, AEC obtains dataless seed files from IRIS.
3. The assessment of station alignment should be done with as many events as possible from as many azimuths as possible, in order to average out the effects of 3D structure (e.g., *Laske and Masters*, 1996; *Ekström and Busby*, 2008; *Hanna and Long*, 2012). We only use one event in this report. However, the misalignments we identify are, for the most part, consistent with those of *Hanna and Long* (2012), who used several events (Section 4).

Summary of previous reports

Previous version of this report are available on the AEC website under “Technical Reports.”

- Version 1, July 5, 2012. Documenting station performance in Alaska based on Love wave from M_w 8.6 earthquake in Alaska. Key metadata problems include misalignment of stations, clock errors, phase response errors, and amplitude response errors. Another significant problem are data gaps within the time series.

The initial data “grabbed” for KDAK.BH1 was spurious (Figure 5) but later okay.

- Version 2, August 16, 2012. Expanded analysis. Re-analysis with updated metadata for the phase response for AT stations (MENT, YKU2, SVW2). Identified that the borehole sensor for KDAK.II had a problem on the BH1 component, but the surface sensor is okay. Newly identified problems are station misalignments for MENT.AT and YKU2.AT.
- Version 3, November 19, 2012 [cited in *Tape et al.* (2013)]. Re-analysis with updated metadata for station alignments (e.g., PAX.AK, PNL.AK).
- Version 4, June 13, 2013. Re-analysis with updated metadata for station alignments: MENT.AT, CCB.AK, PS10.PS, PS12.PS, TRF.AK. Also, the XZ network (STEEP) was changed to AK.
- Version 5, January 27, 2014. Included HH channels, represented by 8 stations: YKW1.CN, YUK5.CN, HYT.CN, YUK7.CN, VIB.CN, PLBC.CN, HARP.AK, AKT.AK. Added Table 6 and Table 9.

Newly identified problems are that from the HH stations, only PLBC.CN is usable. The other stations have gaps (Figure 7) or other problems, though this might be specific to the waveforms received at AEC. The latest metadata (e.g., Figure 12) now suggest a misalignment for MDM.AK and SKN.AK for the 2012-04-11 epoch (Table 7).

1 Stations not in operation

Table 1 shows the fraction of “active” stations (as of 11-April-2012) that do **not** provide waveforms. This fraction is listed as B/N in the last column. Quote from AEC: “Spring is probably the time when we have the most stations out. They tend to drop out over the winter, and in most cases we can’t start bringing them back until May.” So in some sense, the April event analyzed here occurred at the worst time of year.

Below is a list of stations that were listed as active but that did not have waveforms. The parenthetical label denotes (“observed inactive stations”/“expected active stations”).

- AK network (29/94):

ANM	ATKA	BWN	CHI	CHUM	CNP	CRQ	CTG	DCPH	FID
GLI	GRIN	GRNC	HIN	HMT	LOGN	MCAR	NIKH	PIN	PTPK
PWL	SGA	SII	SSP	SWD	TGL	TNA	WAX	YAH	

- PS network (0/11)
- AT network (1/14): TTA
- AV network (22/28):

AKBB	AKGG	AKLV	AKMO	AKSA	AMKA	KAKN	OKCE	OKFG	OKNC
OKSO	RDDF	RDJH	RDSO	RDWB	RED	SPBG	SPCG	SPCN	SPCR
SPNN	SSBA								

- CN network (54/66):

BCBC	BMBC	BPCB	BTB	BVCY	CBB	CPLB	DIB	EDB	EDM
EUNU	FHRB	FNBB	HOLB	HOPB	LLLB	LZB	MGB	MOBC	MWAB
NLLB	OZB	PA01	PA02	PA03	PA04	PA05	PA12	PACB	PFB
PGC	PHC	PNT	RES	RUBB	SHB	SLEB	SNB	SOKB	SPLB
TLCB	TOFB	UBRB	VGZ	WALA	WSLR	YKW2	YKW4	YOUB	YUK1
YUK2	YUK3	YUK4	YUK6						

Among these CN stations, the only one with data at IRIS (but not AEC) is EUNU, and it appears to have major gaps over the time interval of interest.

- US network (0/2)
- IU network (2/4): ADK, BILL
- II network (0/1)
- PP network (1/1): GCSA

2 Selection and processing of seismograms

We analyzed the waveforms from the 2012-April-11 M_w 8.6 Sumatra earthquake. In Alaska the dominant waveform from the Sumatra earthquake was the Love wave, which had a dominant period of 130 s and a peak-to-peak displacement exceeding 4 cm (median 4.3 cm). The group velocity across Alaska was 4.5 km/s and therefore the wavelength is approximately 585 km. This long-wavelength Love wave is relatively insensitive to the structural complexity in Alaska associated with active subduction tectonics, and it therefore provides an opportunity to check stations for possible errors associated with timing (clocks), orientation (i.e., alignment), and instrument response to ground motion.

Seismograms and station metadata were obtained from the the Alaska Earthquake Information Center. All stations within an arc distance of 25° of a point in central Alaska. Processing and analysis was done in Matlab using the GISMO Suite (*Reyes and West, 2011*). The instrument responses were deconvolved from all raw time series using the bandpass 0.5 s to 500 s. More problems arise if the cutoff period is lengthened to 1000 s, especially on the 120 s Trillium instruments. (See Table 3 for a list of instruments.) This is not surprising, as deconvolution may amplify low-signal, long-wavelengths for stations with lower corner periods.

Here we list some of the different types of inferred errors in the metadata for stations in Alaska. Some of these can be identified in the transverse component seismograms in Figures 13–17 or in the zoomed-in versions in Figures 18–22.

1. **Misalignment of stations.** Due to the consistency of the Sumatra Love wave across Alaska, (Figure 2), we are able to identify stations with suspected misalignment (Section 4).
2. **Clock error.** Two stations, NCT.AV and TABL.AK, had known clock errors that were awaiting servicing at the time of the earthquake. These stations were not excluded since their waveforms appear to be accurate. We applied clock corrections of 50 s (NCT) and 200 s (TABL) prior to the analysis; this is needed to isolate the approximate time window of the Love wave.
3. **Phase response error.** Version 1 of the report identified phase response errors (of nearly 180° at periods 100–150 s) at MENT.AT, YKU2.AT, and SVW2.AT. Associated metadata have since been corrected.
4. **Amplitude response error.** In other cases (e.g., DOT.AK, DIV.AK) the waveforms look similar to the other 86 stations in mainland Alaska, (Figure 2), but the amplitude of the Love wave differs by at least $\pm 10\%$ (this will depend on the frequency), which in this case cannot be explained by structural effects.

3 Thresholding stations for scientific analysis

Thresholding of waveforms for analysis reduces the initial set of **115 stations** to 86 stations (Figure 2).

3.1 115 to 113: Eliminating (2) records without three components

The COR.IU waveforms for horizontal components are available at IRIS but not at AEC.

- COR.IU, IL31.IM

3.2 113 to 104: Eliminating (9) records with data gaps

Several time series were unusable due to the presence of data gaps (e.g., Figure 6); a complete list is shown in Table 6. Figure 8 shows the spatial pattern. The proximity of gap-stations to non-gap stations suggests that the problem is station-specific, rather than due to external effects (such as inclement weather). For example, three (formerly XZ) stations within a dense cluster in south east Alaska (GOAT.AK, BERG.AK, BARK.AK) have gaps, but no stations around them do. OHAK.AT has gaps, but adjacent KDAK.II does not; AKUT.AT has gaps, but adjacent AKRB.AV does not.

There is no obvious relationship between data gaps and the type of instrument (Table 3).

- GOAT.AK, BERG.AK, BARK.AK have data gaps.
- AKUT.AT, SDPT.AT, OHAK.AT, CHGN.AT have data gaps (Figure 6).
- ILBB.XM has data gaps and looks really odd.
- SPIA.AK has data gaps and is noisy (all three components).

3.3 104 to 100: Eliminating (4) “odd-looking records”

The borehole station for KDAK.II.BH1 was not usable, but the surface station channel SH1 was usable (Figure 9).

- SIT.AT east component is super noisy.
- PS01.PS north component is garbage.
- KABU.AV waveform is too dissimilar; also a long-period notch at ~ 2000 s (Figure 17).
- PS07.PS has no seismometer, but there is a data stream.

3.4 100 to 93: Eliminating (7) records based on suspected instrument response errors (amplitude or phase)

- DIV.AK has wrong amplitude response (too high). (Figure 21)

`cmg3esp_30sec+dm24@50`

- DOT.AK has wrong amplitude response (too low). (Figure 19)

`cmg3esp_30sec+dm24@50`

Version 1: DOT.AK has wrong amplitude response (too high).

- FALS.AK has wrong amplitude response (too high). (Figure 22)

`cmg3esp_30sec+q330_1b100c@50`

- GAMB.AK amplitude is too high. (Figure 22)

`cmg3esp_30sec+q330_1b100c@50`

- MID.AT has an odd phase and low amplitude. (Figure 22)

(Yun Wang, a postdoc at UAF, has examined amplitude patterns for hundreds of events from 2009–2011. She also identified anomalously low amplitudes at MID from events arriving from all directions. Based on this, we believe that the amplitude response is incorrect, or at least too low.)

- YKW3.CN amplitude is too large. (Figure 18)

Version 1: YKW3.CN Love waveform is dissimilar from others (might be structural effects), and the vertical is pure noise. (Figure 18)

- DAWY.CN waveform is dissimilar from others (might be structural effects). (Figure 18)

3.5 93 to 86: Eliminating (7) HH records based on gaps or other problems

In Version 5 of this report, I included stations with HH channels, in addition to the BH channels from before. This resulted in using 8 additional stations in the analysis: YKW1.CN, YUK5.CN, HYT.CN, YUK7.CN, VIB.CN, PLBC.CN, HARP.AK, AKT.AK. All but PLBC.CN are unusable, mainly due to data gaps (Figure 7). It is possible that the waveforms for CN stations are AEC are bad, while the “final” waveforms for these stations are okay. I cannot easily check this, since the waveforms of interest are not available at the IRIS DMC.

- YKW1.CN, YUK5.CN, YUK7.CN, and HYT.CN all have data gaps (Figure 7).
- VIB.CN is garbage.
- AKT.AK is garbage.
- HARP.AK has garbage horizontal components.

3.6 Other problematic records that should probably be cut

- As shown in Table 7, the following stations have suspected misalignments $> 20^\circ$: YKU2.AT and COLD.AK. These stations should not be used for a scientific analysis that uses the horizontal component waveforms. These stations were excluded from Figure 1.
- NCT.AV and SPCP.AV are clearly too low in amplitude (Figure 3); so is MSW.AV (2.3 cm), which is the lowest among all 86 stations. These are all CMG-6TD-T6054.4 response files. These might benefit from a cutoff period shorter than 500 s.

AKRB.AV is also CMG-6TD-T6054.4 but has a “normal” amplitude — if anything, too high (4.6 cm) for where it is located relative to maximal recorded displacements.

SPCP.AV has a long-period notch at ~ 2000 s (Figure 17).

- BBB.CN peak-to-peak amplitude of 5.34 cm is anomalously high (largest among 86 stations), especially considering its large epicentral distance (where geometrical spreading should lead to a decreased amplitude). The waveform is quite dissimilar, but it is also far from the other stations. It also has a subtle (240 points long), late data gap.

Figure 22

4 Station misalignments

A seismic station is aligned to a particular azimuth (ϕ'), but this direction may not be identical to the angle that is associated with the station metadata (ϕ). This angular discrepancy, $\Delta\phi = \phi - \phi'$, represents a misalignment of the station, and fortunately these can be corrected either by reorienting the station by $\Delta\phi$ or by changing the metadata from ϕ to $\phi = \phi'$. Several different techniques can be used to identify station misalignments: global surface wave propagation (*Laske and Masters, 1996; Ekström and Busby, 2008*), ambient noise cross correlation, regional waveform modeling (*Tape et al., 2010*), and shear-wave splitting (*Hanna and Long, 2012*). For example, *Laske and Masters (1996)* found significant misalignments of 3–16 degrees at 12 of 76 GSN (II, IU) and Geoscope (G) stations.

Due to the consistency of the Sumatra Love wave across Alaska (Figures 2 and 3), we are able to identify stations with suspected misalignment. *Hanna and Long (2012)* (HL2012) provided a table of alignment corrections; however, these corrections are only valid at some particular time period (epoch) for each station. Therefore, we examine the time history for the horizontal alignment entry, `hang`, for all stations in the analysis (Figure 12). In some cases (e.g., DOT, PNL, DIV), HL2012 report a misalignment, and `hang` has changed within the past few months or years, so we do not apply their correction. In other cases (e.g., WRH.AK; Figure 12d) `hang` has never changed over the life of the station, so we apply the correction of HL2012. Our resultant list of corrections is in Table 5.

Table 7 contains information comparing the apparent deviation of the Sumatra Love wave from a great-circle path. Because the Love wave is the largest waveform from Sumatra, we simply compute a horizontal vector associated with the absolute value of the maximum horizontal displacement. We then compare the azimuthal angle of this vector with the azimuthal angle associated with the transverse component, which is perpendicular to the station back-azimuth angle. We also performed a polarization analysis on the Love waveforms to ensure that the max horizontal displacement azimuth is a good approximation for the polarization vector. Two example stations are shown in Figures 10 and 11. For all 86 stations, the standard deviation between the two different estimates for the azimuthal angle is 1.6° , which is much less than the inferred misalignment angles (e.g., Figure 4 and Table 7).

In Table 7 we make the calculations assuming no HL2012 corrections, then next assuming the corrections in Table 5. Here we explain a couple stations to clarify what is in Table 7. With respect to the Sumatra epicenter, the positive transverse component for TRF.AK points toward 205.5° ; its negative transverse component points to 25.5° . For a 1D Earth, the maximum horizontal displacement would be in one of these two directions. **The following numbers are no longer true, since the TRF alignment metadata changed between v. 3 and v. 4. (Therefore the HL2012 correction is no longer applied.)** For the Sumatra Love wave, the max displacement is in the direction of 49.3° , which deviates by 23.9° from the transverse component. Assuming the -22° correction of HL2012 (we add this number to the `hang` field), the max displacement is in the direction of 27.3° , which deviates by 1.9° from the transverse component. In other words, after the HL2012 correction is applied, we have a discrepancy of 1.9° ; without the correction, the discrepancy is 23.9° .

Other stations, like PS06.PS and MLY.AK, were not analyzed by HL2012. For these stations, Table 7 could be used as the primary guide for identifying station misalignments. (Until a more rigorous analysis is performed, e.g., *Ekström and Busby (2008)*.)

There are two physical reasons why the Love wave arrival angle could differ from its great-circle path. First, the Love wave could have been deflected from its path by very large-scale

structure, like the transition between continental lithosphere and oceanic lithosphere. In this case we might expect that all deviations would be systematically positive or negative. Second, it is possible that regional structure might influence the arrival angle. However, the Love wave here has a wavelength of approximately 585 km and is therefore only sensitive to relatively large-scale regional structures.

Figures 4 and 5 explore the patterns in the apparent deviation angles of the Love wave. We make three observations:

1. Figure 4 shows that there is a wide spread of deviation angles, and there are no strong spatial correlations to suggest that structure is the primary cause (Figure 5). Therefore, we hypothesize that the spread of angles is primarily due to installation errors.
2. Applying the HL2012 corrections eliminates some of the outliers and clusters more values near 0° (Figure 4). This gives us confidence that the Sumatra Love wave is identifying the same misalignments as the HL2012 SKS splitting measurements. (However, one station Table 7, HOM.AK, has much larger deviations for Sumatra after applying the HL2012 correction.)
3. There is a suggestion of predominantly positive deviation angles: Figure 4b shows a median of 3.2° and a mean 5.5° . From Figure 5 there is a tendency for $\sim 10^\circ$ positive deviations for stations with lower azimuthal angles from Sumatra (TOLK, FYU, EGAK, PS06, GLM, COLA, MDM), but there are also counter-examples (PS05, CCB, WRH, MLY).

Note that almost all of the STEEP stations (southeastern Alaska)—which were similar instruments installed over a relatively short time period—are within $\pm 5^\circ$. This suggests that where stations are installed in a consistent fashion, the station alignments tend to be more accurate. In summary, I believe that the primary source of the spread of deviation angles is due to errors in station installation or errors in metadata (including the possibility of instrument response).

5 Results by network

Results by network are summarized with the ratios in Table 1. Three ratios are listed:

- A/B , the fraction of waveform-producing stations that were used for scientific purposes
- A/N , the fraction of “active” stations that were used for scientific purposes
- B/N , the fraction of “active” stations that produced waveforms (usable or not)

The ratio A/B is the fraction of stations that was used for scientific purposes. The ratio A/N is the fraction of “active” stations that provided waveforms, whether usable for scientific analysis or not. For example, in the region of interest there are four network-IU stations, two of which provide waveforms (COLA, COR) two of which do not (ADK, BILL).

6 Recommendations for networks in Alaska and for the AEC database of waveforms and metadata

These recommendations are in approximate order of importance:

1. Check station alignments, wherever possible. Our results in Table 5 (see also previous report versions) corroborate the corrections listed by *Hanna and Long* (2012), with only one exception (HOM.AK). Note that Table 5 examined only a subset of the total stations in operation.

Figure 5 suggests a systematic deflection of the Sumatra Love wave from its great circle path, which is indicated by the angular discrepancies $\Delta\phi = 5^\circ - 15^\circ$ for stations north of about 63° latitude. Given this pattern and the stations listed in Table 5, I consider the stations with the “most suspect” alignments **for the station epoch containing 2012-04-11** (note ¹) to be

- YKU2.AT (-32°)
- MLY.AK (-18°)
- WRH.AK (-15°); also Hanna and Long
- UNV.AK (-15°); also Hanna and Long
- MENT.AT (-7°); surrounded by 6 stations with $\Delta\phi$ between 0° and 10° (Figure 5)
- CRAG.AT (-11°); nearby WRAK.US is 4° , which is consistent with all the STEEP stations
- MCK.AK (18°); also Hanna and Long
- SKN.AK (27°); surrounding stations are between -5° and 10° (Figure 5)
- MDM.AK (24°); surrounding stations (except WRH and MLY) are between 0° (CCB, 0.5°) and 15° (GLM, 13.3°) (Figure 5)

(Note that these estimates are only approximate, since they are based on the analysis of one earthquake.)

MDM.AK and SKN.AK are new to this list in Version 5; Figure 12 shows how the horizontal alignment had changed with time, according to the latest metadata.

2. Consider applying corrections to metadata based on detailed surface wave analysis (e.g., *Ekström and Busby*, 2008). For example, a station like SKN.AK, which has been visited multiple times since 2012-04-11 (Figure 12), may have the correct metadata now, but incorrect metadata for 2012-04-11 (or some particular epoch). Using teleseismic surface waves for events during that epoch, one could probably demonstrate that the station alignment metadata is incorrect. Such a procedure could be applied to retroactively correct metadata — at least in the most extreme cases where misalignment of $|\Delta\phi| > 10^\circ$ is identified.
3. Check the amplitude responses for the stations identified here.

For the AK network, DIV, DOT, FALS, and GAMB are all Guralp CMG3 instruments, suggesting a problem with the CMG3 metadata being used.

¹A suspected misalignment here does not mean that the current alignment value in the metadata is incorrect, since the epoch could have changed since the epoch containing 2012-04-11.

4. Minimize data gaps (e.g., Figure 6, Table 6). These appear to be station-specific problems (Section 3.2), since gap-stations are adjacent to non-gap-stations for this analysis.
5. Determine why there are pervasive gaps in the HH stations (Section 3.5). I have seen scientific results that use the same records, but without gaps, so the gaps seem specific to AEC waveforms. (Note that several CN stations do not have waveforms available at IRIS, e.g., Figure 7.)
6. Check all stations for clock errors. Two identified here, NCT.AV and TABL.AK, had conspicuously large timing errors (>50 s) or “clock shifts.” But there could be subtler errors (<5 s). Clock errors will have a detrimental impact on tomography studies, since arrival times will incorporate the clock error, which will then be incorrectly mapped onto source or structure errors in the tomographic inversion.

Stehly et al. (2007) showed how ambient noise analysis could be used to identify “significant instrumental time errors (0.5 s)” in the southern California network. Such an analysis—continuously running—would be valuable for any network, it seems.

7. Provide an easy-to-identify log-tracking system for any updates to the metadata in `master_stations`. An example is shown in Table 2.
8. Provide location codes KDAK.II and COLA.IU that are consistent with IRIS convention. For example, for this event there are these broadband channels:

TOLK.TA	BHZ	BHE	BHN	--	BHZ_01	BHE_01	BHN_01
WRAK.US	BHZ	BH1	BH2	--	BHZ_10	BH1_10	BH2_10
COLA.IU	BHZ	BH1	BH2	--	SHZ	SH1	SH2
KDAK.II	BHZ	BH1	BH2	--	SHZ	SH1	SH2

It would be simpler to eliminate the in-house use of the SH channel for COLA and KDAK, since there are other multi-sensor stations (like TOLK and WRAK) that are left with the IRIS convention.

9. Provide horizontal components for COR.IU (and all other non-AK stations), if possible. This request is aimed at allowing UAF/GI users to not make a separate request to IRIS DMC for waveforms (and metadata). But it is important that the waveforms at AEC are the “final” versions available at IRIS.

Finally, it would obviously be great to have waveforms from stations that are listed as active (Section 1).

Related questions

1. Are there standards set forth by IRIS (or AEC) for measuring alignment? What measurement devices are used?
2. Are data gaps “permanent”? In other words, is it possible to recover information that is missing in the digital waveforms? (Figure 6)

Acknowledgments

Many thanks to Natasha Ruppert for feedback on this report and for helping to improve the metadata for the Alaska Seismic Network. Thanks to Yun Wang for feedback on this report and for developing scripts to interact with the continuous waveform database. Thanks to Michael West for the polarization analysis scripts (Figures 10 and 11), which build upon the Waveform Toolbox (*Reyes and West, 2011*).

References

- Ekström, G., and R. W. Busby (2008), Measurements of seismometer orientation at USArray Transportable Array and backbone stations, *Seis. Res. Lett.*, *79*(4), 554–561.
- Hanna, J., and M. D. Long (2012), SKS splitting beneath Alaska: Regional variability and implications for subduction processes at a slab edge, *Tectonophysics*, *530-531*, 272–285.
- Laske, G., and G. Masters (1996), Constraints on global phase velocity maps from long-period polarization data, *J. Geophys. Res.*, *101*(B7), 16,059–16,075.
- Reyes, C. G., and M. E. West (2011), The Waveform Suite: A robust platform for manipulating waveforms in MATLAB, *Seis. Res. Lett.*, *82*, 104–110.
- Stehly, L., M. Campillo, and N. M. Shapiro (2007), Traveltime measurements from noise correlation: stability and detection of instrumental time-shifts, *Geophys. J. Int.*, *171*, 223–230.
- Tape, C., Q. Liu, A. Maggi, and J. Tromp (2010), Seismic tomography of the southern California crust based on spectral-element and adjoint methods, *Geophys. J. Int.*, *180*, 433–462.
- Tape, C., M. West, V. Silwal, and N. Ruppert (2013), Earthquake nucleation and triggering on an optimally oriented fault, *Earth Planet. Sci. Lett.*, *363*, 231–241.

Table 1: Networks in Alaska for the stations in this analysis. The region of stations is a circular cap with radius 25° , centered on interior Alaska (lon -148.95° , lat 64.92°). Networks are listed in order of the number stations used for scientific analysis (A). A is the number of stations with waveforms usable for scientific analysis. B is the number of stations with waveforms available. N is the number of stations listed as active in the database. PP.GCSA will eventually migrate to the AK network. (The network code PS officially belongs to the POSEIDON network.) (The borehole station for KDAK.II was unusable, but the surface station was usable: Figure 9.)

Network	code	A	B	N	A/B	A/N	B/N
Alaska Regional Network	AK	56	65	94	0.86	0.60	0.69
“Pump Station”	PS*	9	11	11	0.82	0.82	1.00
Alaska Tsunami Warning Seismic System	AT	7	13	14	0.54	0.50	0.93
Canadian National Seismic Network	CN	5	12	66	0.42	0.08	0.18
Alaska Volcano Observatory	AV	4	6	28	0.67	0.14	0.21
US National Seismic Network	US	2	2	2	1.00	1.00	1.00
IRIS/USGS Network	IU	1	2	4	0.50	0.25	0.50
IRIS/IDA Network	II	1	1	1	1.00	1.00	1.00
USArray Transportable Array	TA	1	1	1	1.00	1.00	1.00
Princeton Earth Physics Program	PP	0	0	1	–	0.00	0.00
TOTAL		86	113	222	0.76	0.39	0.51

Table 2: Suggested table for tracking dataless seed updates in the AEC `master_stations` database. See Table 1 for names of networks. The dates of IRIS dataless seed files at IRIS were last checked on 17-Nov-2012. (Table from Version 3 report.)

Network	file name	file date at IRIS	IRIS file date in MS	date of last MS update	MS update needed?
AK	AK.dataless	23-Oct-2012	–	–	–
AT	AT.dataless	06-Aug-2012	???	03-Aug-2012	Y
AV	AV.dataless	25-Aug-2012	???	27-Sept-2012	N
CN	CN.dataless	06-Aug-2012	???	03-Aug-2012	Y
II	II.dataless	10-Nov-2012	???	??	??
IU	IU.dataless	13-Nov-2012	??	??	??
TA	TA.dataless	14-Nov-2012	??	16-Oct-2012	Y
US	US.dataless	19-Sept-2012	??	24-Aug-2011	Y
XZ	XZ.2005-2012.dataless	10-Oct-2012	–	–	–

Table 3: First part of 112 stations with three components available. The azimuth and distance, both in degrees, are measured with respect to the offshore Sumatra event (92.78° , 2.24°).

AKRB	AV	az	35.30	dist	94.71	lon	-166.0708	lat	54.1292	CMG-6TD-T6054.4
AKT	AV	az	35.26	dist	94.88	lon	-165.7720	lat	54.1349	cmg40t_30sec+dm24@100
AKUT	AT	az	35.26	dist	94.88	lon	-165.7719	lat	54.1352	STS-2:Trident.1
BAGL	AK	az	24.61	dist	104.48	lon	-142.0915	lat	60.4896	trillium_240_2+q330_lb100c@50
BAL	AK	az	24.21	dist	104.08	lon	-142.3462	lat	61.0360	trillium_120+q330_lb100c@50
BARK	AK	az	24.80	dist	104.36	lon	-142.4931	lat	60.4030	trillium_240_2+q330_lb100c@50
BARN	AK	az	24.00	dist	104.35	lon	-141.6622	lat	61.0595	trillium_240_2+q330_lb100c@50
BBB	CN	az	26.43	dist	115.69	lon	-128.1133	lat	52.1847	Guralp_CMG3T_120sec:CNSN_GD2_v.4
BCP	AK	az	24.38	dist	105.80	lon	-139.6369	lat	59.9534	trillium_120+q330_lb100c@50
BERG	AK	az	25.13	dist	103.85	lon	-143.7038	lat	60.3923	trillium_120+q330_lb100c@50
BESE	AK	az	23.99	dist	108.58	lon	-134.8559	lat	58.5792	trillium_240_2+q330_lb100c@50
BGLC	AK	az	25.26	dist	104.17	lon	-143.2841	lat	60.1205	trillium_120+q330_lb100c@50
BMR	AK	az	24.86	dist	103.18	lon	-144.6051	lat	60.9677	cmg3t_120sec+dm24@50
BPAW	AK	az	23.42	dist	99.11	lon	-150.9873	lat	64.0997	trillium_240_2+q330_lb100c@50
BRLK	AK	az	27.42	dist	100.96	lon	-150.9063	lat	59.7511	sts2_g3+q330_lb100c@50
CAST	AK	az	24.25	dist	98.94	lon	-152.0844	lat	63.4188	trillium_240_2+q330_lb100c@50
CCB	AK	az	22.30	dist	100.10	lon	-147.8053	lat	64.6453	trillium_240_2+q330_lb100c@50
CHGN	AT	az	32.12	dist	98.45	lon	-158.4142	lat	56.3014	STS-2:Trident.1
COLA	IU	az	22.11	dist	99.97	lon	-147.8616	lat	64.8736	Geotech_KS-54000_Borehole_Sei.35
COLD	AK	az	20.42	dist	98.05	lon	-150.2038	lat	67.2269	cmg3t_120sec+q330_lb100c@50
CRAG	AT	az	25.91	dist	111.29	lon	-133.1230	lat	55.4689	STS-2:Trident.1
DAWY	CN	az	20.84	dist	103.51	lon	-139.3909	lat	64.0655	Guralp_CMG3ESP_60sec:CNSN_GD2.15
DHY	AK	az	23.62	dist	101.01	lon	-147.3759	lat	63.0753	trillium_240_2+q330_lb100c@50
DIV	AK	az	25.00	dist	102.60	lon	-145.7749	lat	61.1292	cmg3esp_60sec+dm24@50
DLBC	CN	az	22.33	dist	110.58	lon	-130.0272	lat	58.4372	Guralp_CMG3T_120sec:CNSN_GD2_v.4
DOT	AK	az	22.36	dist	102.01	lon	-144.0697	lat	63.6482	cmg3esp_30sec+dm24@50
EGAK	US	az	20.69	dist	102.47	lon	-141.1581	lat	64.7774	STS2-I=80414=Gen=Q330SR=0742.1
EYAK	AK	az	25.51	dist	102.90	lon	-145.7500	lat	60.5487	cmg3t_120sec+dm24@50
FALS	AK	az	34.27	dist	96.08	lon	-163.4175	lat	54.8564	cmg3esp_30sec+q330_lb100c@50
FIB	AK	az	25.96	dist	100.69	lon	-150.1775	lat	61.1656	trillium_120+q330_lb100c@50
FYU	AK	az	20.07	dist	100.09	lon	-145.2342	lat	66.5657	trillium_120+q330_lb100c@50
GAMB	AK	az	26.16	dist	90.42	lon	-171.7035	lat	63.7758	cmg3esp_60sec+q330_lb100c@50
GHO	AK	az	25.14	dist	100.97	lon	-148.9260	lat	61.7710	trillium_120+q330_lb100c@50
GLM	AK	az	21.91	dist	100.09	lon	-147.3999	lat	64.9878	trillium_120+q330_lb100c@50
GOAT	AK	az	25.23	dist	103.32	lon	-144.7292	lat	60.5805	trillium_240_2+q330_lb100c@50
HARP	AK	az	23.72	dist	102.23	lon	-145.1567	lat	62.3986	cmg3esp_60sec+dm24@100
HDA	AK	az	22.34	dist	100.54	lon	-146.9477	lat	64.4095	trillium_240_2+q330_lb100c@50
HOM	AK	az	27.67	dist	100.65	lon	-151.6515	lat	59.6572	trillium_120+q330_lb100c@50
HYT	CN	az	23.00	dist	106.14	lon	-137.5038	lat	60.8250	Guralp_CMG3ESP_NSN:Taurus_Inf.40
INK	CN	az	15.92	dist	102.67	lon	-133.5254	lat	68.3065	Guralp_CMG3T_120sec:CNSN_GD2_.43
ISLE	AK	az	24.58	dist	104.31	lon	-142.3406	lat	60.6024	trillium_240_2+q330_lb100c@50
JIS	AK	az	24.07	dist	108.97	lon	-134.3848	lat	58.2758	trillium_120+q330_lb100c@50
KABU	AV	az	29.69	dist	99.42	lon	-155.2843	lat	58.2702	CMG-6TD-T6054.80
KAI	AK	az	25.73	dist	103.78	lon	-144.4188	lat	59.9268	trillium_120+q330_lb100c@50
KDAK	II	az	29.62	dist	100.94	lon	-152.5835	lat	57.7828	Streckeisen_STS-2_Seismometer.86
KHIT	AK	az	24.97	dist	104.02	lon	-143.2510	lat	60.4427	trillium_240_2+q330_lb100c@50
KIAG	AK	az	24.31	dist	104.13	lon	-142.3605	lat	60.9231	trillium_240_2+q330_lb100c@50
KLU	AK	az	24.71	dist	102.36	lon	-145.9227	lat	61.4924	trillium_240_2+q330_lb100c@50
KNK	AK	az	25.37	dist	101.33	lon	-148.4585	lat	61.4131	trillium_120+q330_lb100c@50
KTH	AK	az	23.91	dist	99.36	lon	-150.9233	lat	63.5527	trillium_240_2+q330_lb100c@50
KULT	AK	az	25.00	dist	104.34	lon	-142.7234	lat	60.2474	trillium_240_2+q330_lb100c@50
MCK	AK	az	23.36	dist	100.08	lon	-148.9373	lat	63.7318	trillium_240_2+q330_lb100c@50
MDM	AK	az	22.11	dist	99.79	lon	-148.2318	lat	64.9602	trillium_120+q330_lb100c@50
MENT	AT	az	22.90	dist	102.52	lon	-143.7194	lat	62.9380	Trillium-240:Trident.2
MESA	AK	az	24.85	dist	104.71	lon	-141.9505	lat	60.1785	trillium_240_2+q330_lb100c@50

Table 4: Part 2 of Table 3.

MID	AT	az	26.67	dist	103.18	lon	-146.3388	lat	59.4278	STS-2:Trident.1
MLY	AK	az	22.52	dist	98.81	lon	-150.7418	lat	65.0303	trillium_240_2+q330_lb100c@50
MSW	AV	az	35.59	dist	94.33	lon	-166.7880	lat	53.9148	CMG-6TD-T6054.143
NCT	AV	az	27.08	dist	99.71	lon	-152.9293	lat	60.5621	CMG-6TD-T6054.149
NICH	AK	az	25.34	dist	103.82	lon	-143.9692	lat	60.2361	trillium_240_2+q330_lb100c@50
OHAK	AT	az	30.29	dist	100.80	lon	-153.2875	lat	57.2225	STS-2:Trident.1
PAX	AK	az	23.29	dist	101.82	lon	-145.4699	lat	62.9699	sts2_g3+q330_lb100c@50
PLBC	CN	az	23.77	dist	107.43	lon	-136.3659	lat	59.4550	Guralp_CMG3T_30sec:CNSN_GD2_v.72
PMR	AT	az	25.35	dist	100.96	lon	-149.1308	lat	61.5922	STS-2:Trident.1
PNL	AK	az	24.55	dist	106.06	lon	-139.4036	lat	59.6659	trillium_240_2+q330_lb100c@50
PPD	AK	az	21.05	dist	100.52	lon	-145.5246	lat	65.5174	trillium_240_2+q330_lb100c@50
PPLA	AK	az	24.76	dist	99.11	lon	-152.1894	lat	62.8962	sts2_g3+q330_lb100c@50
PS01	PS	az	17.43	dist	97.18	lon	-148.6139	lat	70.2580	cmg3t_120sec+q330_lb100c@50
PS04	PS	az	19.20	dist	97.80	lon	-149.3568	lat	68.4215	cmg3t_120sec+q330_lb100c@50
PS05	PS	az	20.88	dist	98.07	lon	-150.6646	lat	66.8133	cmg3esp_60sec+q330_lb100c@50
PS06	PS	az	21.59	dist	98.82	lon	-149.7370	lat	65.8545	cmg40t_30sec+q330_lb100c@50
PS07	PS	az	21.80	dist	99.61	lon	-148.2816	lat	65.3101	cmg3esp_60sec+q330_lb100c@50
PS08	PS	az	22.19	dist	100.52	lon	-146.8220	lat	64.5421	cmg3esp_60sec+q330_lb100c@50
PS09	PS	az	22.51	dist	101.22	lon	-145.7682	lat	63.9299	cmg3esp_60sec+q330_lb100c@50
PS10	PS	az	22.96	dist	101.47	lon	-145.7707	lat	63.4229	cmg3t_100sec+q330_lb100c@50
PS11	PS	az	24.08	dist	102.26	lon	-145.4752	lat	62.0788	cmg3esp_60sec+q330_lb100c@50
PS12	PS	az	24.54	dist	102.70	lon	-145.1459	lat	61.4749	cmg3esp_60sec+q330_lb100c@50
RAG	AK	az	25.39	dist	103.44	lon	-144.6773	lat	60.3863	sts2_g3+q330_lb100c@50
RC01	AK	az	25.94	dist	100.92	lon	-149.7390	lat	61.0890	cmg3esp_60sec+dm24@50
RDOG	AK	az	21.32	dist	93.22	lon	-162.9080	lat	68.0541	trillium_240_2+q330_lb100c@50
RIDG	AK	az	22.46	dist	101.67	lon	-144.8440	lat	63.7403	sts2_g3+q330_lb100c@50
RKAV	AK	az	24.57	dist	104.89	lon	-141.3478	lat	60.2994	sts2_g3+q330_lb100c@50
RND	AK	az	23.64	dist	100.26	lon	-148.8602	lat	63.4056	sts2_g3+q330_lb100c@50
SAMH	AK	az	24.56	dist	105.22	lon	-140.7828	lat	60.1294	trillium_240_2+q330_lb100c@50
SAW	AK	az	24.98	dist	101.20	lon	-148.3318	lat	61.8070	trillium_240_2+q330_lb100c@50
SCM	AK	az	24.73	dist	101.61	lon	-147.3296	lat	61.8329	trillium_240_2+q330_lb100c@50
SCRK	AK	az	22.06	dist	101.87	lon	-143.9882	lat	63.9765	sts2_g3+q330_lb100c@50
SDPT	AT	az	33.38	dist	97.60	lon	-160.4766	lat	55.3493	STS-2:Trident.4
SIT	AT	az	25.41	dist	109.34	lon	-135.3244	lat	57.0569	STS-2:Trident.6
SKAG	AT	az	23.43	dist	107.84	lon	-135.3290	lat	59.4601	STS-2:Trident.4
SKN	AK	az	25.48	dist	99.76	lon	-151.5317	lat	61.9800	sts2_g3+q330_lb100c@50
SMY	AT	az	37.20	dist	82.97	lon	174.1031	lat	52.7308	STS-2:Trident.6
SPCP	AV	az	26.27	dist	99.78	lon	-152.1550	lat	61.2655	CMG-6TD-T6054.178
SPIA	AK	az	32.65	dist	91.90	lon	-170.2477	lat	57.1766	cmg3esp_60sec+dm24@50
SSN	AK	az	25.81	dist	100.32	lon	-150.7467	lat	61.4636	sts2_g3+q330_lb100c@50
SUCK	AK	az	25.44	dist	103.99	lon	-143.7790	lat	60.0720	trillium_120+q330_lb100c@50
SVW2	AT	az	27.05	dist	98.28	lon	-155.6217	lat	61.1082	Trillium-240:Trident.10
TABL	AK	az	24.39	dist	104.90	lon	-141.1443	lat	60.4399	trillium_240_2+q330_lb100c@50
TOLK	TA	az	19.04	dist	97.63	lon	-149.5724	lat	68.6408	Guralp_CMG3T:Quanterra_330_Li.17
TRF	AK	az	23.89	dist	99.66	lon	-150.2893	lat	63.4502	cmg3esp_60sec+dm24@50
UNV	AK	az	35.62	dist	94.51	lon	-166.5040	lat	53.8456	cmg3esp_60sec+dm24@50
VIB	CN	az	27.51	dist	112.97	lon	-132.5406	lat	53.2522	Guralp_CMG3T_120sec:CNSN_GD2.100
VMT	PS	az	25.19	dist	102.37	lon	-146.3694	lat	61.0827	cmg3esp_60sec+q330_lb100c@50
VRDI	AK	az	24.33	dist	103.52	lon	-143.4545	lat	61.2275	trillium_240_2+q330_lb100c@50
WHY	CN	az	22.30	dist	107.25	lon	-134.8806	lat	60.6597	Guralp_CMG3ESP_NSN:CNSN_GD1_d.80
WRAK	US	az	24.83	dist	111.01	lon	-132.3466	lat	56.4191	STS2-I=80404=Gen=Q330SR=1366.5
WRH	AK	az	22.52	dist	100.07	lon	-148.0916	lat	64.4715	trillium_240_2+q330_lb100c@50
YKU2	AT	az	24.76	dist	106.03	lon	-139.6710	lat	59.5121	Trillium-240:Trident.10
YKW1	CN	az	13.21	dist	112.13	lon	-114.4843	lat	62.4822	Guralp_CMG3ESP_NSN:CNSN_GD2_.108
YKW3	CN	az	13.22	dist	112.03	lon	-114.6099	lat	62.5616	Streckeisen_STS-1:CNSN_Yello.110
YUK5	CN	az	22.85	dist	105.82	lon	-137.8593	lat	61.1315	Guralp_CMG3ESP_60sec:Taurus_.115
YUK7	CN	az	23.44	dist	106.07	lon	-138.1399	lat	60.5307	Guralp_CMG3ESP_60sec:Taurus_.115

Table 5: Station misalignments in *Hanna and Long* (2012) that were applied in this analysis. We applied only the (non-zero) alignment corrections in HL2012 for stations whose horizontal alignment metadata had **not** changed prior to 2014-01-21. See Version 3 for a list of corrections that were applied for the analysis of *Tape et al.* (2013).

station	longitude	latitude	angle
WRH	-148.09	64.47	18.0
UNV	-166.50	53.85	12.0
HOM	-151.65	59.66	-10.0
MCK	-148.94	63.73	-10.0
SAW	-148.33	61.81	-9.0
RIDG	-144.84	63.74	-7.0

Table 6: Records with data gaps. The station list is AKT, AKUT, BARK, BBB, BERG, CHGN, EYAK, GOAT, HYT, IL31, ILBB, KABU, OHAK, SDPT, SKAG, SPCP, SPIA, YKW1, YKW3, YUK5, YUK7. Stations EYAK, BBB, SKAG, SPCP were kept within the analysis, despite having small gaps that could have an effect. (The filtered records of SPCP and BBB were cut to avoid the influence of the gaps.) Note that filtering seismograms that have gaps will generally lead to spurious results.

start time 2012-04-11 08:41:57, end time 2012-04-11 10:21:57

AKUT AT BHZ ngaps =	264424
BARK AK BHZ ngaps =	280424
BBB CN BHZ ngaps =	240
BERG AK BHZ ngaps =	276076
CHGN AT BHZ ngaps =	78556
GOAT AK BHZ ngaps =	261250
IL31 IM BHZ ngaps =	96698
ILBB XM BHZ ngaps =	10680
KABU AV BHZ ngaps =	500
OHAK AT BHZ ngaps =	91872
SDPT AT BHZ ngaps =	46006
SPIA AK BHZ ngaps =	78300
YKW3 CN BHZ ngaps =	5960
AKUT AT BHE ngaps =	261746
BARK AK BHE ngaps =	280424
BBB CN BHE ngaps =	240
BERG AK BHE ngaps =	276076
CHGN AT BHE ngaps =	78148
EYAK AK BHE ngaps =	450
GOAT AK BHE ngaps =	261250
ILBB XM BHE ngaps =	10480
OHAK AT BHE ngaps =	91790
SDPT AT BHE ngaps =	46486
SPIA AK BHE ngaps =	73850
YKW3 CN BHE ngaps =	1080
AKUT AT BHN ngaps =	264472
BARK AK BHN ngaps =	280424
BBB CN BHN ngaps =	240
BERG AK BHN ngaps =	276076
CHGN AT BHN ngaps =	77720
GOAT AK BHN ngaps =	261250
ILBB XM BHN ngaps =	10520
KABU AV BHN ngaps =	1500
OHAK AT BHN ngaps =	92522
SDPT AT BHN ngaps =	46468
SKAG AT BHN ngaps =	500
SPCP AV BHN ngaps =	500
SPIA AK BHN ngaps =	82700
YKW3 CN BHN ngaps =	5960
AKT AV HHZ ngaps =	2
HYT CN HHZ ngaps =	323144
YKW1 CN HHZ ngaps =	19600
YUK5 CN HHZ ngaps =	236344
YUK7 CN HHZ ngaps =	258744
AKT AV HHE ngaps =	2
HYT CN HHE ngaps =	331344
YKW1 CN HHE ngaps =	13200
YUK5 CN HHE ngaps =	243600
YUK7 CN HHE ngaps =	245544
AKT AV HHN ngaps =	2
HYT CN HHN ngaps =	320000
YKW1 CN HHN ngaps =	29000
YUK5 CN HHN ngaps =	240400

Table 7: Angular deviation of max horizontal vector from transverse component for the 86 stations used for scientific analysis (Figure 2). **Misalignments at the non-86 stations might also be possible.** The stations are sorted in order from maximum to minimum angular deviation, without any corrections applied. The first set of numbers following GC refer to great-circle directions: the back-azimuth (**baz**), the azimuth of the positive transverse component (**Tp**), and the azimuth of the negative transverse component (**Tn**). The number following CT is the azimuthal direction of the maximum horizontal displacement, followed by its deviation from the transverse component. The numbers following HL are the same, but with the *Hanna and Long* (2012) (Table 5) corrections applied. In all cases except one (HOM), the angular deviation decreases after applying the correction.

YKU2	AT	GC:	baz	304.6	Tp	214.6	Tm	34.6	//	CT:	2.3	(-32.3)				
SKN	AK	GC:	baz	294.1	Tp	204.1	Tm	24.1	//	CT:	51.1	(27.0)				
MDM	AK	GC:	baz	297.6	Tp	207.6	Tm	27.6	//	CT:	51.2	(23.6)				
COLD	AK	GC:	baz	296.1	Tp	206.1	Tm	26.1	//	CT:	49.3	(23.3)				
MCK	AK	GC:	baz	296.8	Tp	206.8	Tm	26.8	//	CT:	45.0	(18.2)	HL:	35.0	(8.2)
MLY	AK	GC:	baz	295.3	Tp	205.3	Tm	25.3	//	CT:	7.4	(-17.9)				
SCM	AK	GC:	baz	297.9	Tp	207.9	Tm	27.9	//	CT:	44.2	(16.2)				
WRH	AK	GC:	baz	297.7	Tp	207.7	Tm	27.7	//	CT:	12.4	(-15.3)	HL:	30.4	(2.7)
UNV	AK	GC:	baz	280.1	Tp	190.1	Tm	10.1	//	CT:	175.0	(-15.2)	HL:	187.0	(-3.2)
GLM	AK	GC:	baz	298.4	Tp	208.4	Tm	28.4	//	CT:	41.8	(13.3)				
COLA	IU	GC:	baz	298.0	Tp	208.0	Tm	28.0	//	CT:	40.5	(12.5)				
PPD	AK	GC:	baz	300.3	Tp	210.3	Tm	30.3	//	CT:	222.7	(12.5)				
RND	AK	GC:	baz	296.8	Tp	206.8	Tm	26.8	//	CT:	38.7	(11.9)				
KTH	AK	GC:	baz	294.9	Tp	204.9	Tm	24.9	//	CT:	36.6	(11.7)				
AKRB	AV	GC:	baz	280.5	Tp	190.5	Tm	10.5	//	CT:	202.2	(11.6)				
CRAG	AT	GC:	baz	309.8	Tp	219.8	Tm	39.8	//	CT:	28.7	(-11.1)				
WHY	CN	GC:	baz	309.5	Tp	219.5	Tm	39.5	//	CT:	50.5	(11.0)				
RDOG	AK	GC:	baz	284.2	Tp	194.2	Tm	14.2	//	CT:	204.2	(10.0)				
SSN	AK	GC:	baz	294.7	Tp	204.7	Tm	24.7	//	CT:	14.9	(-9.9)				
EGAK	US	GC:	baz	304.3	Tp	214.3	Tm	34.3	//	CT:	223.3	(9.0)				
FIB	AK	GC:	baz	295.2	Tp	205.2	Tm	25.2	//	CT:	34.2	(9.0)				
DHY	AK	GC:	baz	298.1	Tp	208.1	Tm	28.1	//	CT:	37.0	(8.9)				
KNK	AK	GC:	baz	296.8	Tp	206.8	Tm	26.8	//	CT:	35.7	(8.9)				
TOLK	TA	GC:	baz	296.8	Tp	206.8	Tm	26.8	//	CT:	215.4	(8.6)				
PS06	PS	GC:	baz	296.3	Tp	206.3	Tm	26.3	//	CT:	34.3	(7.9)				
PLBC	CN	GC:	baz	307.8	Tp	217.8	Tm	37.8	//	CT:	45.6	(7.8)				
PMR	AT	GC:	baz	296.2	Tp	206.2	Tm	26.2	//	CT:	33.9	(7.6)				
PS11	PS	GC:	baz	299.7	Tp	209.7	Tm	29.7	//	CT:	37.3	(7.6)				
PAX	AK	GC:	baz	299.9	Tp	209.9	Tm	29.9	//	CT:	37.1	(7.3)				
RIDG	AK	GC:	baz	300.6	Tp	210.6	Tm	30.6	//	CT:	37.8	(7.2)	HL:	30.8	(0.2)
MENT	AT	GC:	baz	301.5	Tp	211.5	Tm	31.5	//	CT:	24.4	(-7.2)				
DLBC	CN	GC:	baz	313.6	Tp	223.6	Tm	43.6	//	CT:	50.7	(7.1)				

Table 8: Part 2 of Table 7.

JIS	AK	GC: baz	309.4	Tp	219.4	Tm	39.4	//	CT:	46.2	(6.9)	
PS04	PS	GC: baz	297.0	Tp	207.0	Tm	27.0	//	CT:	213.8	(6.8)	
PS08	PS	GC: baz	298.9	Tp	208.9	Tm	28.9	//	CT:	35.5	(6.6)	
SPCP	AV	GC: baz	293.4	Tp	203.4	Tm	23.4	//	CT:	16.8	(-6.6)	
CAST	AK	GC: baz	293.8	Tp	203.8	Tm	23.8	//	CT:	30.1	(6.3)	
FYU	AK	GC: baz	300.7	Tp	210.7	Tm	30.7	//	CT:	36.9	(6.2)	
HDA	AK	GC: baz	298.7	Tp	208.7	Tm	28.7	//	CT:	34.9	(6.1)	
MESA	AK	GC: baz	302.6	Tp	212.6	Tm	32.6	//	CT:	38.4	(5.7)	
BBB	CN	GC: baz	313.6	Tp	223.6	Tm	43.6	//	CT:	49.3	(5.6)	
PS12	PS	GC: baz	299.9	Tp	209.9	Tm	29.9	//	CT:	35.4	(5.5)	
SAW	AK	GC: baz	297.0	Tp	207.0	Tm	27.0	//	CT:	32.4	(5.4)	HL: 23.4 (-3.6)
PS10	PS	GC: baz	299.7	Tp	209.7	Tm	29.7	//	CT:	34.7	(5.0)	
SAMH	AK	GC: baz	303.7	Tp	213.7	Tm	33.7	//	CT:	38.7	(5.0)	
SVW2	AT	GC: baz	290.3	Tp	200.3	Tm	20.3	//	CT:	15.9	(-4.3)	
SKAG	AT	GC: baz	308.7	Tp	218.7	Tm	38.7	//	CT:	42.9	(4.2)	
KLU	AK	GC: baz	299.2	Tp	209.2	Tm	29.2	//	CT:	33.2	(4.0)	
WRAK	US	GC: baz	310.8	Tp	220.8	Tm	40.8	//	CT:	44.8	(4.0)	
RKAV	AK	GC: baz	303.2	Tp	213.2	Tm	33.2	//	CT:	37.1	(3.9)	
KULT	AK	GC: baz	301.9	Tp	211.9	Tm	31.9	//	CT:	28.1	(-3.8)	
PS05	PS	GC: baz	295.6	Tp	205.6	Tm	25.6	//	CT:	21.8	(-3.7)	
BCP	AK	GC: baz	304.8	Tp	214.8	Tm	34.8	//	CT:	38.5	(3.7)	
KDAK	II	GC: baz	292.5	Tp	202.5	Tm	22.5	//	CT:	18.8	(-3.7)	
PPLA	AK	GC: baz	293.6	Tp	203.6	Tm	23.6	//	CT:	27.3	(3.6)	
NCT	AV	GC: baz	292.6	Tp	202.6	Tm	22.6	//	CT:	19.4	(-3.2)	
BMR	AK	GC: baz	300.3	Tp	210.3	Tm	30.3	//	CT:	33.5	(3.2)	
KIAG	AK	GC: baz	302.4	Tp	212.4	Tm	32.4	//	CT:	35.6	(3.2)	
EYAK	AK	GC: baz	299.2	Tp	209.2	Tm	29.2	//	CT:	31.8	(2.6)	
BAL	AK	GC: baz	302.4	Tp	212.4	Tm	32.4	//	CT:	35.0	(2.6)	
RC01	AK	GC: baz	295.6	Tp	205.6	Tm	25.6	//	CT:	28.1	(2.5)	
PS09	PS	GC: baz	299.8	Tp	209.8	Tm	29.8	//	CT:	32.3	(2.5)	
KAI	AK	GC: baz	300.3	Tp	210.3	Tm	30.3	//	CT:	32.8	(2.5)	
KHIT	AK	GC: baz	301.5	Tp	211.5	Tm	31.5	//	CT:	33.9	(2.5)	
INK	CN	GC: baz	312.3	Tp	222.3	Tm	42.3	//	CT:	224.8	(2.5)	
VMT	PS	GC: baz	298.7	Tp	208.7	Tm	28.7	//	CT:	31.1	(2.4)	
BARN	AK	GC: baz	303.1	Tp	213.1	Tm	33.1	//	CT:	35.4	(2.4)	
BRLK	AK	GC: baz	294.3	Tp	204.3	Tm	24.3	//	CT:	22.0	(-2.3)	
RAG	AK	GC: baz	300.1	Tp	210.1	Tm	30.1	//	CT:	32.3	(2.2)	
TRF	AK	GC: baz	295.5	Tp	205.5	Tm	25.5	//	CT:	23.3	(-2.1)	
SCRK	AK	GC: baz	301.5	Tp	211.5	Tm	31.5	//	CT:	33.6	(2.1)	
PNL	AK	GC: baz	304.9	Tp	214.9	Tm	34.9	//	CT:	36.9	(2.0)	
BESE	AK	GC: baz	309.0	Tp	219.0	Tm	39.0	//	CT:	40.9	(2.0)	
TABL	AK	GC: baz	303.4	Tp	213.4	Tm	33.4	//	CT:	35.4	(1.9)	
BPAW	AK	GC: baz	294.9	Tp	204.9	Tm	24.9	//	CT:	26.6	(1.7)	
MSW	AV	GC: baz	279.9	Tp	189.9	Tm	9.9	//	CT:	191.0	(1.1)	
VRDI	AK	GC: baz	301.4	Tp	211.4	Tm	31.4	//	CT:	32.5	(1.1)	
SMY	AT	GC: baz	264.6	Tp	174.6	Tm	354.6	//	CT:	175.6	(1.0)	
BGLC	AK	GC: baz	301.4	Tp	211.4	Tm	31.4	//	CT:	30.4	(-1.0)	
BAGL	AK	GC: baz	302.6	Tp	212.6	Tm	32.6	//	CT:	33.5	(0.9)	
ISLE	AK	GC: baz	302.4	Tp	212.4	Tm	32.4	//	CT:	33.2	(0.9)	
HOM	AK	GC: baz	293.6	Tp	203.6	Tm	23.6	//	CT:	24.3	(0.7)	HL: 14.3 (-9.3)
CCB	AK	GC: baz	298.0	Tp	208.0	Tm	28.0	//	CT:	28.5	(0.5)	
SUCK	AK	GC: baz	300.9	Tp	210.9	Tm	30.9	//	CT:	31.3	(0.4)	
GHO	AK	GC: baz	296.5	Tp	206.5	Tm	26.5	//	CT:	26.0	(-0.4)	
NICH	AK	GC: baz	300.8	Tp	210.8	Tm	30.8	//	CT:	30.5	(-0.3)	

Table 9: Comparison between “top 10” measured misalignments for each version of this report. The list changes because the station metadata for the epoch containing 2012-04-11 changes with time, as newly detected corrections are applied retroactively to earlier time periods. (The notation for Version 1 was different from the following versions.)

VERSION 1																	
COLD	AK	(Tp	206.1	Tm	26.1)	58.5	(32.4)	HL:	43.5	(17.4)					
PS12	PS	(Tp	209.9	Tm	29.9)	61.4	(31.5)	HL:	61.4	(31.5)					
PAX	AK	(Tp	209.9	Tm	29.9)	3.1	(-26.7)	HL:	21.1	(-8.7)					
TRF	AK	(Tp	205.5	Tm	25.5)	49.3	(23.9)	HL:	27.3	(1.9)					
CAST	AK	(Tp	203.8	Tm	23.8)	2.1	(-21.7)	HL:	14.1	(-9.7)					
PS10	PS	(Tp	209.7	Tm	29.7)	49.7	(20.0)	HL:	49.7	(20.0)					
MCK	AK	(Tp	206.8	Tm	26.8)	45.0	(18.2)	HL:	35.0	(8.2)					
MLY	AK	(Tp	205.3	Tm	25.3)	7.4	(-17.9)	HL:	7.4	(-17.9)					
SCM	AK	(Tp	207.9	Tm	27.9)	44.2	(16.2)	HL:	44.2	(16.2)					
PNL	AK	(Tp	214.9	Tm	34.9)	18.9	(-16.0)	HL:	18.9	(-16.0)					
PS06	PS	(Tp	206.3	Tm	26.3)	42.3	(15.9)	HL:	42.3	(15.9)					
WRH	AK	(Tp	207.7	Tm	27.7)	12.4	(-15.3)	HL:	30.4	(2.7)					
UNV	AK	(Tp	190.1	Tm	10.1)	175.0	(-15.2)	HL:	187.0	(-3.2)					
SSN	AK	(Tp	204.7	Tm	24.7)	9.9	(-14.9)	HL:	6.9	(-17.9)					
KTH	AK	(Tp	204.9	Tm	24.9)	39.6	(14.7)	HL:	39.6	(14.7)					
VERSION 2																	
MENT	AT	GC:	baz	301.5	Tp	211.5	Tm	31.5	//	CT:	354.4	(-37.2)				
YKU2	AT	GC:	baz	304.6	Tp	214.6	Tm	34.6	//	CT:	2.3	(-32.3)				
COLD	AK	GC:	baz	296.1	Tp	206.1	Tm	26.1	//	CT:	58.3	(32.3)	HL:	43.3	(17.3)
PS12	PS	GC:	baz	299.9	Tp	209.9	Tm	29.9	//	CT:	61.4	(31.5)				
PAX	AK	GC:	baz	299.9	Tp	209.9	Tm	29.9	//	CT:	3.1	(-26.7)	HL:	21.1	(-8.7)
TRF	AK	GC:	baz	295.5	Tp	205.5	Tm	25.5	//	CT:	49.3	(23.9)	HL:	27.3	(1.9)
CAST	AK	GC:	baz	293.8	Tp	203.8	Tm	23.8	//	CT:	2.1	(-21.7)	HL:	14.1	(-9.7)
PS10	PS	GC:	baz	299.7	Tp	209.7	Tm	29.7	//	CT:	49.7	(20.0)				
MCK	AK	GC:	baz	296.8	Tp	206.8	Tm	26.8	//	CT:	45.0	(18.2)	HL:	35.0	(8.2)
MLY	AK	GC:	baz	295.3	Tp	205.3	Tm	25.3	//	CT:	7.4	(-17.9)				
SCM	AK	GC:	baz	297.9	Tp	207.9	Tm	27.9	//	CT:	44.2	(16.2)				
PNL	AK	GC:	baz	304.9	Tp	214.9	Tm	34.9	//	CT:	18.9	(-16.0)				
PS06	PS	GC:	baz	296.3	Tp	206.3	Tm	26.3	//	CT:	42.3	(15.9)				
WRH	AK	GC:	baz	297.7	Tp	207.7	Tm	27.7	//	CT:	12.4	(-15.3)	HL:	30.4	(2.7)
UNV	AK	GC:	baz	280.1	Tp	190.1	Tm	10.1	//	CT:	175.0	(-15.2)	HL:	187.0	(-3.2)
VERSION 3																	
MENT	AT	GC:	baz	301.5	Tp	211.5	Tm	31.5	//	CT:	354.4	(-37.2)				
YKU2	AT	GC:	baz	304.6	Tp	214.6	Tm	34.6	//	CT:	2.3	(-32.3)				
COLD	AK	GC:	baz	296.1	Tp	206.1	Tm	26.1	//	CT:	58.3	(32.3)				
PS12	PS	GC:	baz	299.9	Tp	209.9	Tm	29.9	//	CT:	61.4	(31.5)				
TRF	AK	GC:	baz	295.5	Tp	205.5	Tm	25.5	//	CT:	49.3	(23.9)	HL:	27.3	(1.9)
CAST	AK	GC:	baz	293.8	Tp	203.8	Tm	23.8	//	CT:	2.1	(-21.7)	HL:	14.1	(-9.7)
PS10	PS	GC:	baz	299.7	Tp	209.7	Tm	29.7	//	CT:	49.7	(20.0)				
MCK	AK	GC:	baz	296.8	Tp	206.8	Tm	26.8	//	CT:	45.0	(18.2)	HL:	35.0	(8.2)
MLY	AK	GC:	baz	295.3	Tp	205.3	Tm	25.3	//	CT:	7.4	(-17.9)				
SCM	AK	GC:	baz	297.9	Tp	207.9	Tm	27.9	//	CT:	44.2	(16.2)				
PS06	PS	GC:	baz	296.3	Tp	206.3	Tm	26.3	//	CT:	42.3	(15.9)				
WRH	AK	GC:	baz	297.7	Tp	207.7	Tm	27.7	//	CT:	12.4	(-15.3)	HL:	30.4	(2.7)
UNV	AK	GC:	baz	280.1	Tp	190.1	Tm	10.1	//	CT:	175.0	(-15.2)	HL:	187.0	(-3.2)
SKN	AK	GC:	baz	294.1	Tp	204.1	Tm	24.1	//	CT:	39.1	(15.0)				
KTH	AK	GC:	baz	294.9	Tp	204.9	Tm	24.9	//	CT:	39.6	(14.7)				
VERSION 4																	
YKU2	AT	GC:	baz	304.6	Tp	214.6	Tm	34.6	//	CT:	2.3	(-32.3)				
COLD	AK	GC:	baz	296.1	Tp	206.1	Tm	26.1	//	CT:	49.3	(23.3)				
CAST	AK	GC:	baz	293.8	Tp	203.8	Tm	23.8	//	CT:	2.1	(-21.7)	HL:	14.1	(-9.7)
MCK	AK	GC:	baz	296.8	Tp	206.8	Tm	26.8	//	CT:	45.0	(18.2)	HL:	35.0	(8.2)
MLY	AK	GC:	baz	295.3	Tp	205.3	Tm	25.3	//	CT:	7.4	(-17.9)				
SCM	AK	GC:	baz	297.9	Tp	207.9	Tm	27.9	//	CT:	44.2	(16.2)				
PS06	PS	GC:	baz	296.3	Tp	206.3	Tm	26.3	//	CT:	42.3	(15.9)				
WRH	AK	GC:	baz	297.7	Tp	207.7	Tm	27.7	//	CT:	12.4	(-15.3)	HL:	30.4	(2.7)
UNV	AK	GC:	baz	280.1	Tp	190.1	Tm	10.1	//	CT:	175.0	(-15.2)	HL:	187.0	(-3.2)
SKN	AK	GC:	baz	294.1	Tp	204.1	Tm	24.1	//	CT:	39.1	(15.0)				
GLM	AK	GC:	baz	298.4	Tp	208.4	Tm	28.4	//	CT:	41.8	(13.3)				
COLA	IU	GC:	baz	298.0	Tp	208.0	Tm	28.0	//	CT:	40.5	(12.5)				
PPD	AK	GC:	baz	300.3	Tp	210.3	Tm	30.3	//	CT:	222.7	(12.5)				
RND	AK	GC:	baz	296.8	Tp	206.8	Tm	26.8	//	CT:	38.7	(11.9)				
KTH	AK	GC:	baz	294.9	Tp	204.9	Tm	24.9	//	CT:	36.6	(11.7)				
VERSION 5																	
YKU2	AT	GC:	baz	304.6	Tp	214.6	Tm	34.6	//	CT:	2.3	(-32.3)				
SKN	AK	GC:	baz	294.1	Tp	204.1	Tm	24.1	//	CT:	51.1	(27.0)				
MDM	AK	GC:	baz	297.6	Tp	207.6	Tm	27.6	//	CT:	51.2	(23.6)				
COLD	AK	GC:	baz	296.1	Tp	206.1	Tm	26.1	//	CT:	49.3	(23.3)				
MCK	AK	GC:	baz	296.8	Tp	206.8	Tm	26.8	//	CT:	45.0	(18.2)	HL:	35.0	(8.2)
MLY	AK	GC:	baz	295.3	Tp	205.3	Tm	25.3	//	CT:	7.4	(-17.9)				
SCM	AK	GC:	baz	297.9	Tp	207.9	Tm	27.9	//	CT:	44.2	(16.2)				
WRH	AK	GC:	baz	297.7	Tp	207.7	Tm	27.7	//	CT:	12.4	(-15.3)	HL:	30.4	(2.7)
UNV	AK	GC:	baz	280.1	Tp	190.1	Tm	10.1	//	CT:	175.0	(-15.2)	HL:	187.0	(-3.2)
GLM	AK	GC:	baz	298.4	Tp	208.4	Tm	28.4	//	CT:	41.8	(13.3)				
COLA	IU	GC:	baz	298.0	Tp	208.0	Tm	28.0	//	CT:	40.5	(12.5)				
PPD	AK	GC:	baz	300.3	Tp	210.3	Tm	30.3	//	CT:	222.7	(12.5)				
RND	AK	GC:	baz	296.8	Tp	206.8	Tm	26.8	//	CT:	38.7	(11.9)				
KTH	AK	GC:	baz	294.9	Tp	204.9	Tm	24.9	//	CT:	36.6	(11.7)				
AKRB	AV	GC:	baz	280.5	Tp	190.5	Tm	10.5	//	CT:	202.2	(11.6)				

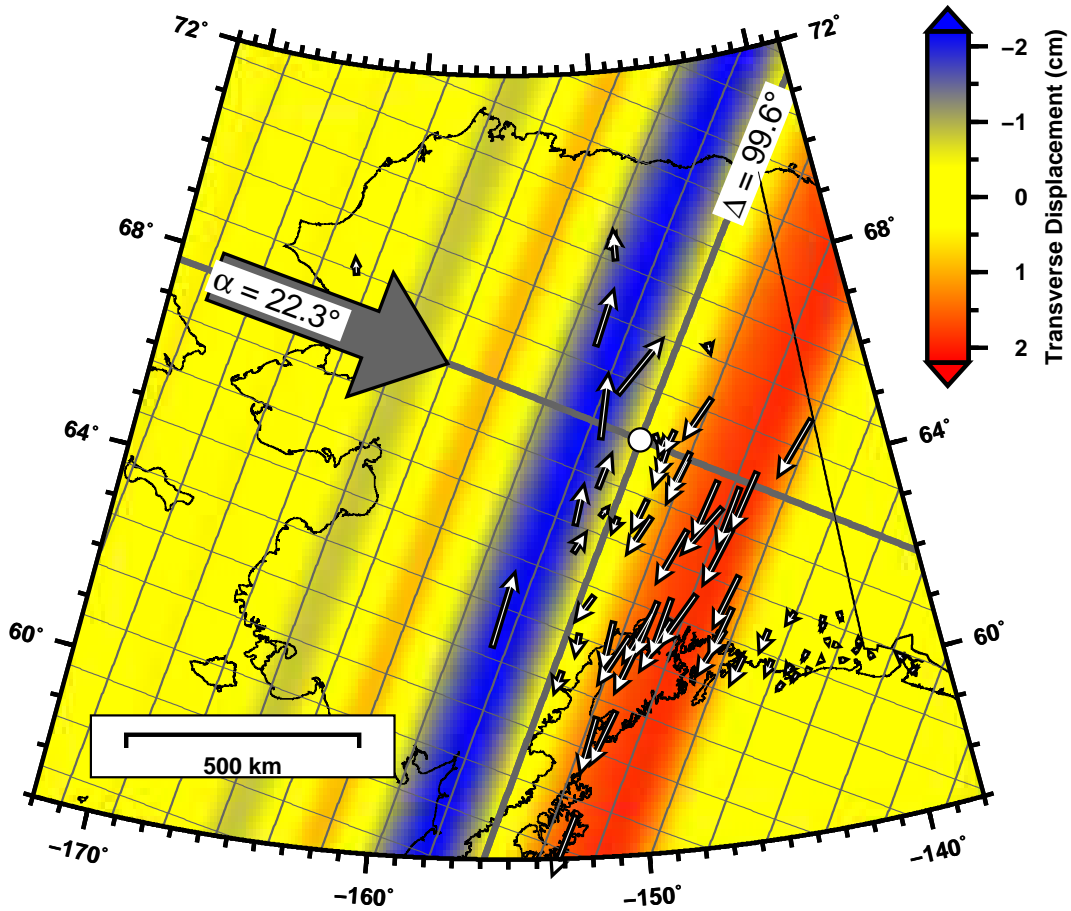


Figure 1: Love waves from the April 11, 2012 M_w 8.6 Sumatra earthquake in Alaska. Horizontal displacement field in Alaska at the origin time of the M_w 3.9 Nenana earthquake in central Alaska (*Tape et al.*, 2013). The epicenter of this event is marked by the white dot at the center of the thick gray lines. The grid lines represent increments of 1° in α and 1° in Δ from the Nenana epicenter. Large deviations from the transverse direction are suggestive of station misalignments.

time aligned on 2012-04-11 09:21:57; INK max 1.91e+07 nm at t = -68.0 s
 BHT HHT SHT [nm, ---] event 201204110838A (2012-04-11, M8.6, 92.8, 2.2, z = 40.0 km)
 43 / 86 seismograms (86 stations) ordered by azimuth, norm ---> none

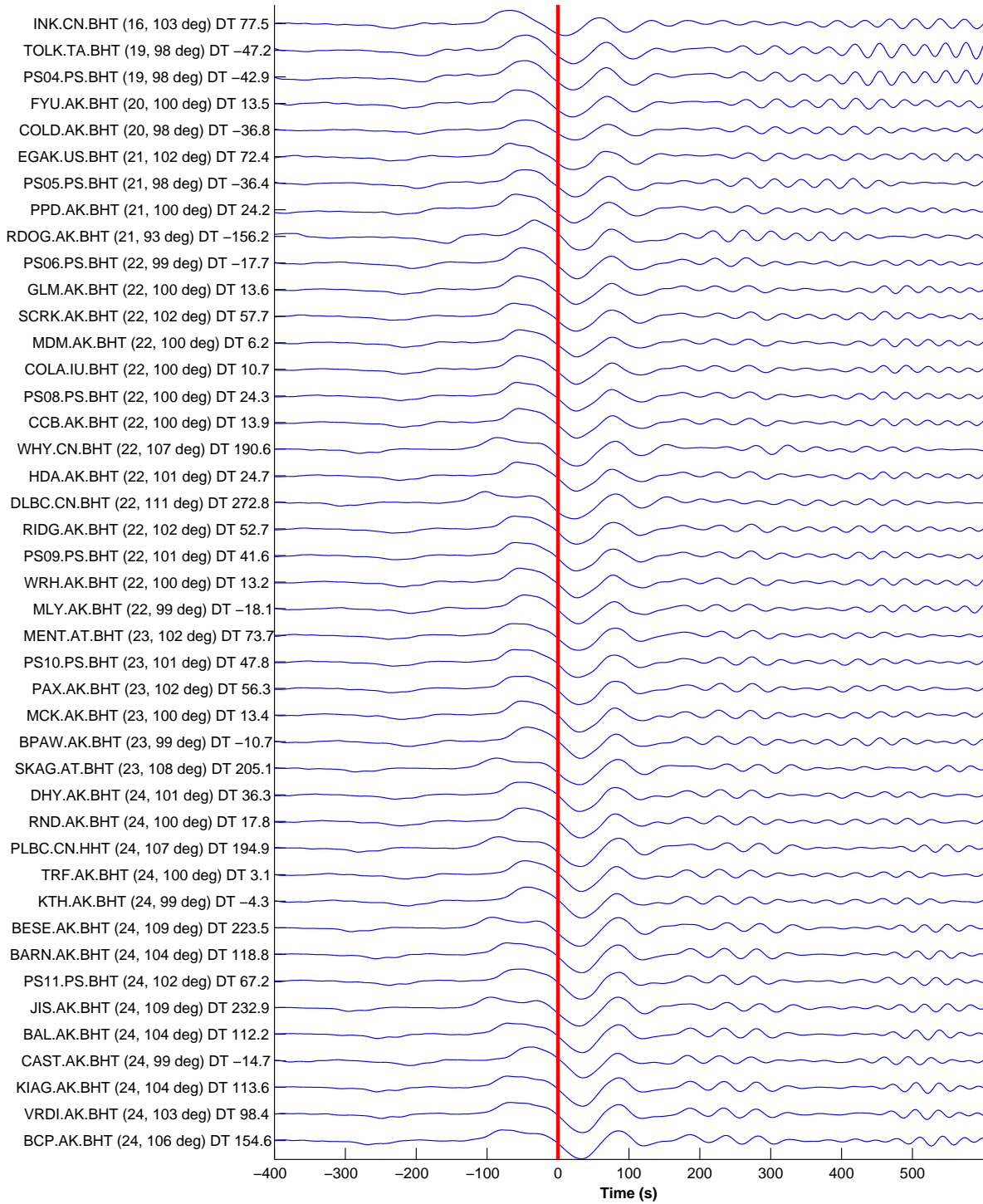
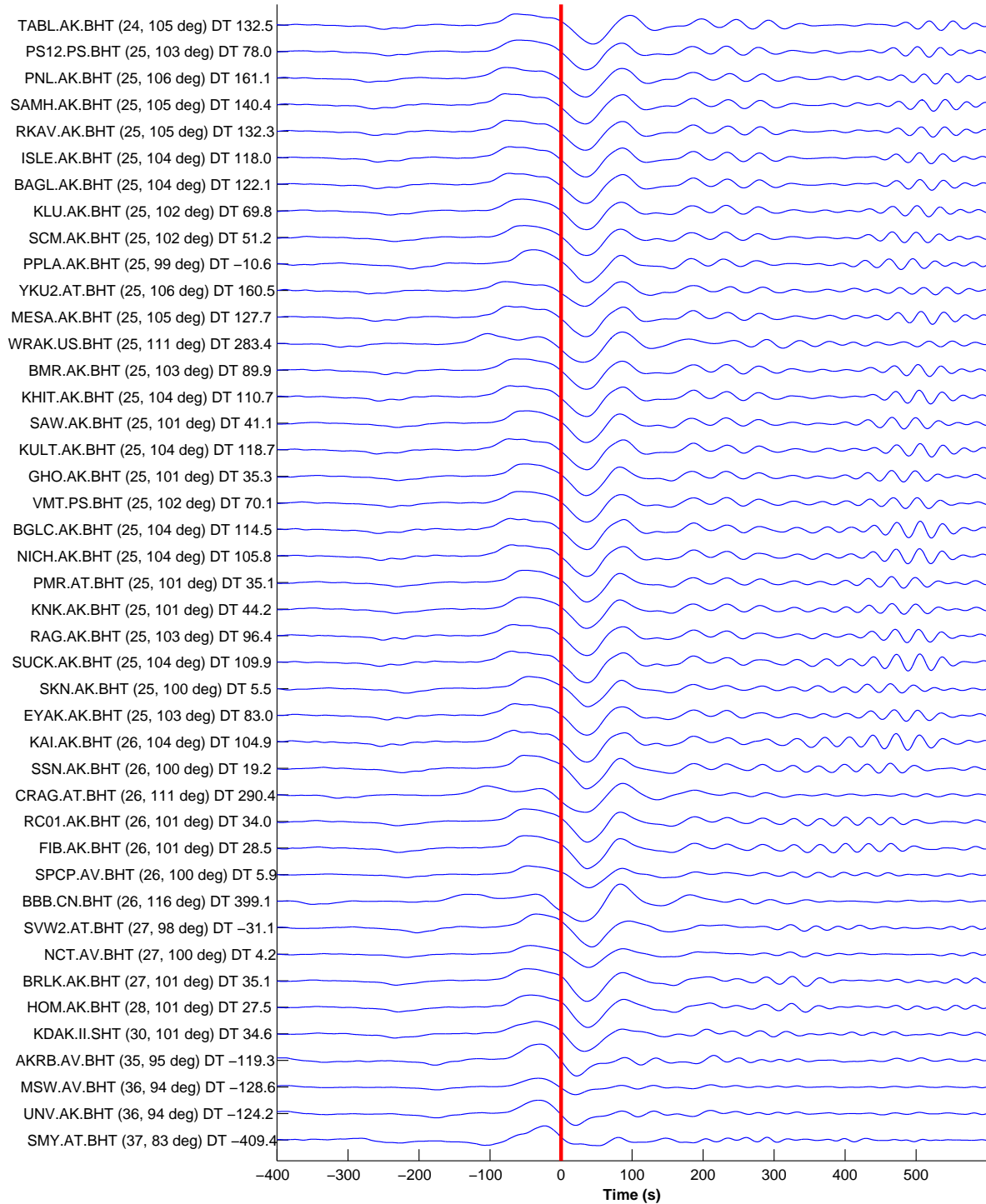


Figure 2: Love waves for all 86 stations used for scientific analysis. (See following page for second half.) Waveforms are plotted as displacement with no relative amplitude scaling. The waveforms are sorted by azimuth, the first number following the station label; the epicentral distance is the second number. Each seismograms has been shifted in time according to its distance from $\Delta = 99.6^\circ$ (Nenana earthquake distance from Sumatra) along its great circle and using a velocity of 4.5 km/s. (They are not aligned by cross correlation, though cross correlation was used to estimate the velocity.) The time shift is labeled as “DT”; for a station on the Sumatra side of $\Delta = 99.6^\circ$, the time shift is negative.

time aligned on 2012-04-11 09:21:57; TABL max $-2.72e+07$ nm at $t = 45.1$ s
BHT HHT SHT [nm, --] event 201204110838A (2012-04-11, M8.6, 92.8, 2.2, z = 40.0 km)
43 / 86 seismograms (86 stations) ordered by azimuth, norm --> none



Second half of Figure 2.

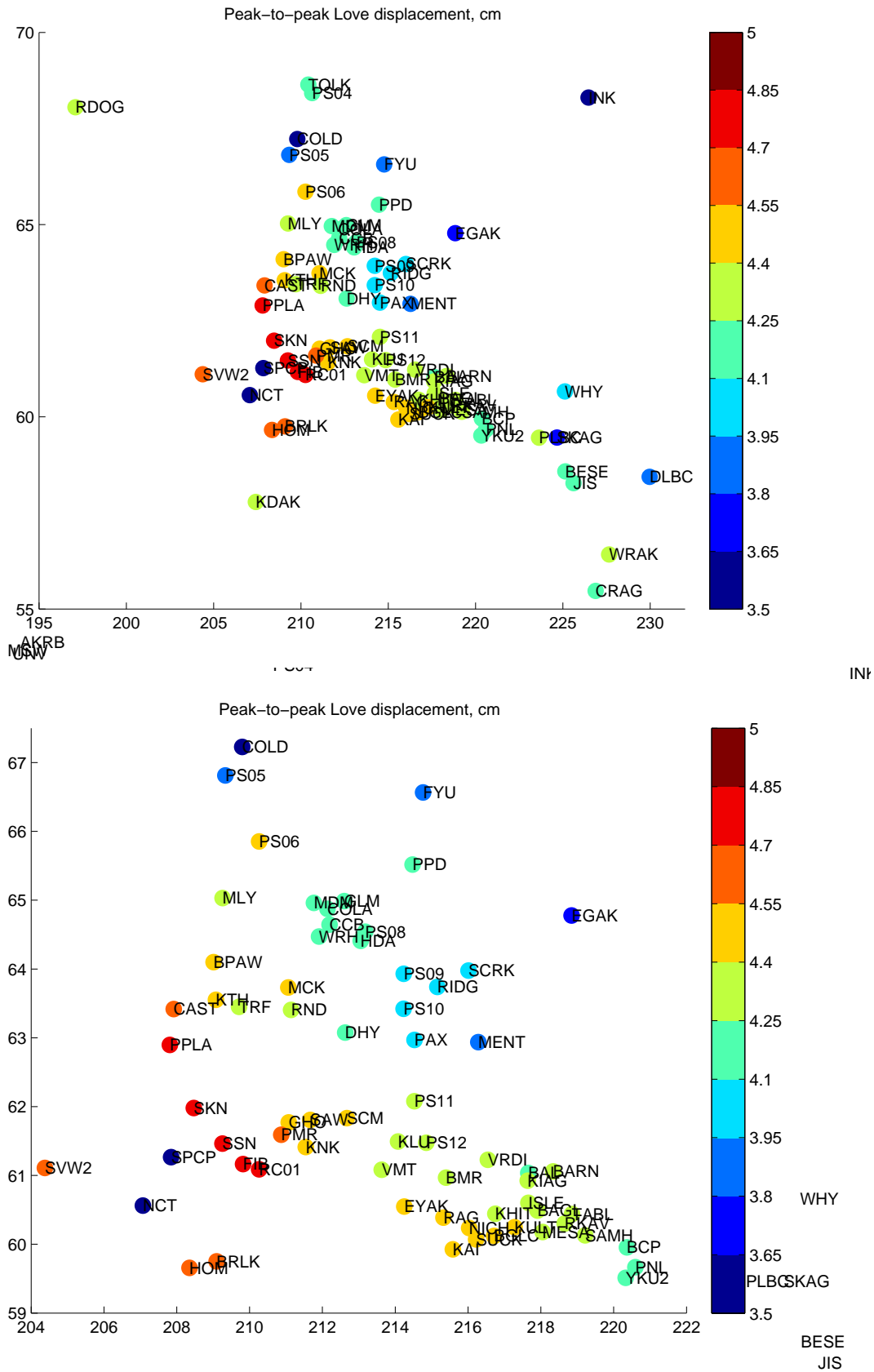


Figure 3: Peak-to-peak horizontal displacements for the Sumatra Love wave, for the 86 stations considered for scientific analysis. Note the outliers NCT.AV and SPCP.AV. Bottom is a zoom-in of the top view.

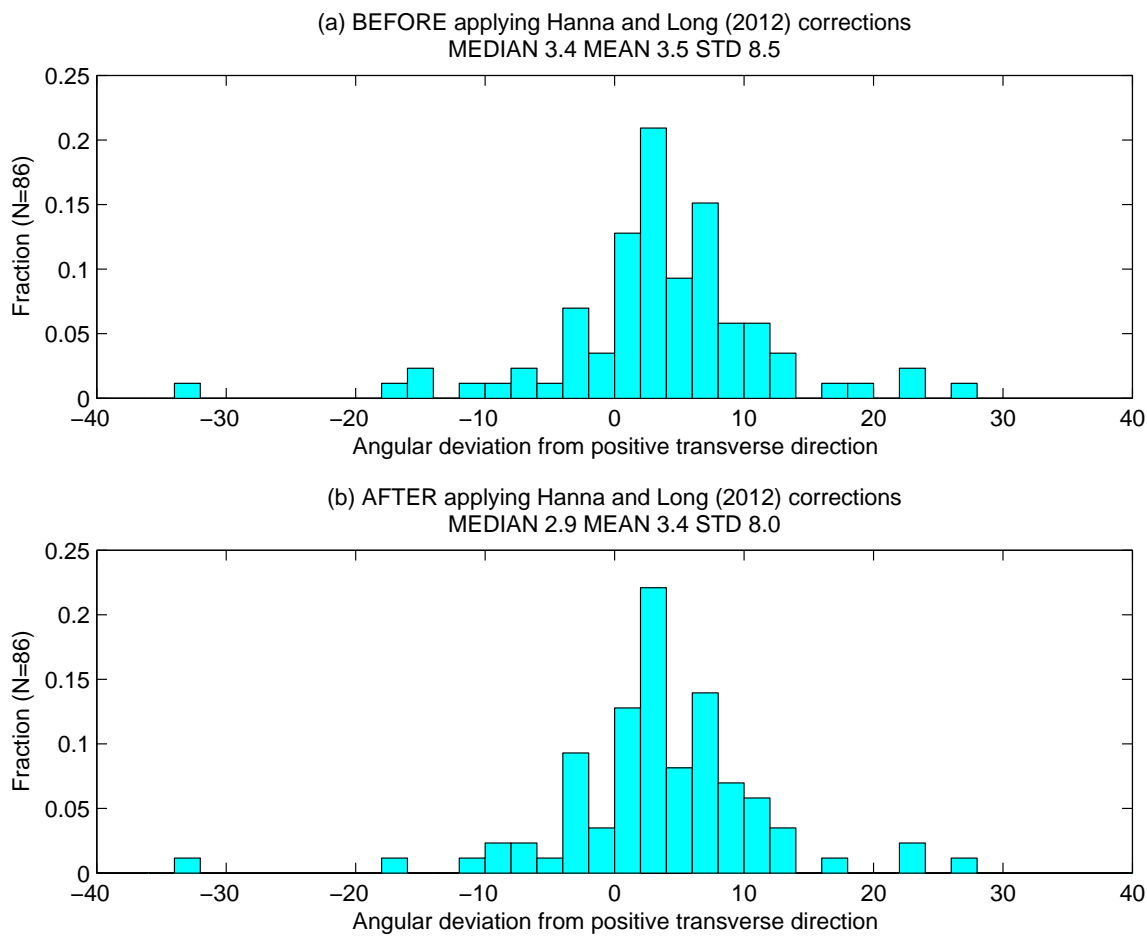


Figure 4: Angular discrepancies between the maximum horizontal displacement from Sumatra (Love wave) and the great-circle transverse component direction. See also Table 7 and Section 4. (a) Before applying corrections of *Hanna and Long* (2012) (Table 5). (b) After applying corrections of *Hanna and Long* (2012) (Table 5).

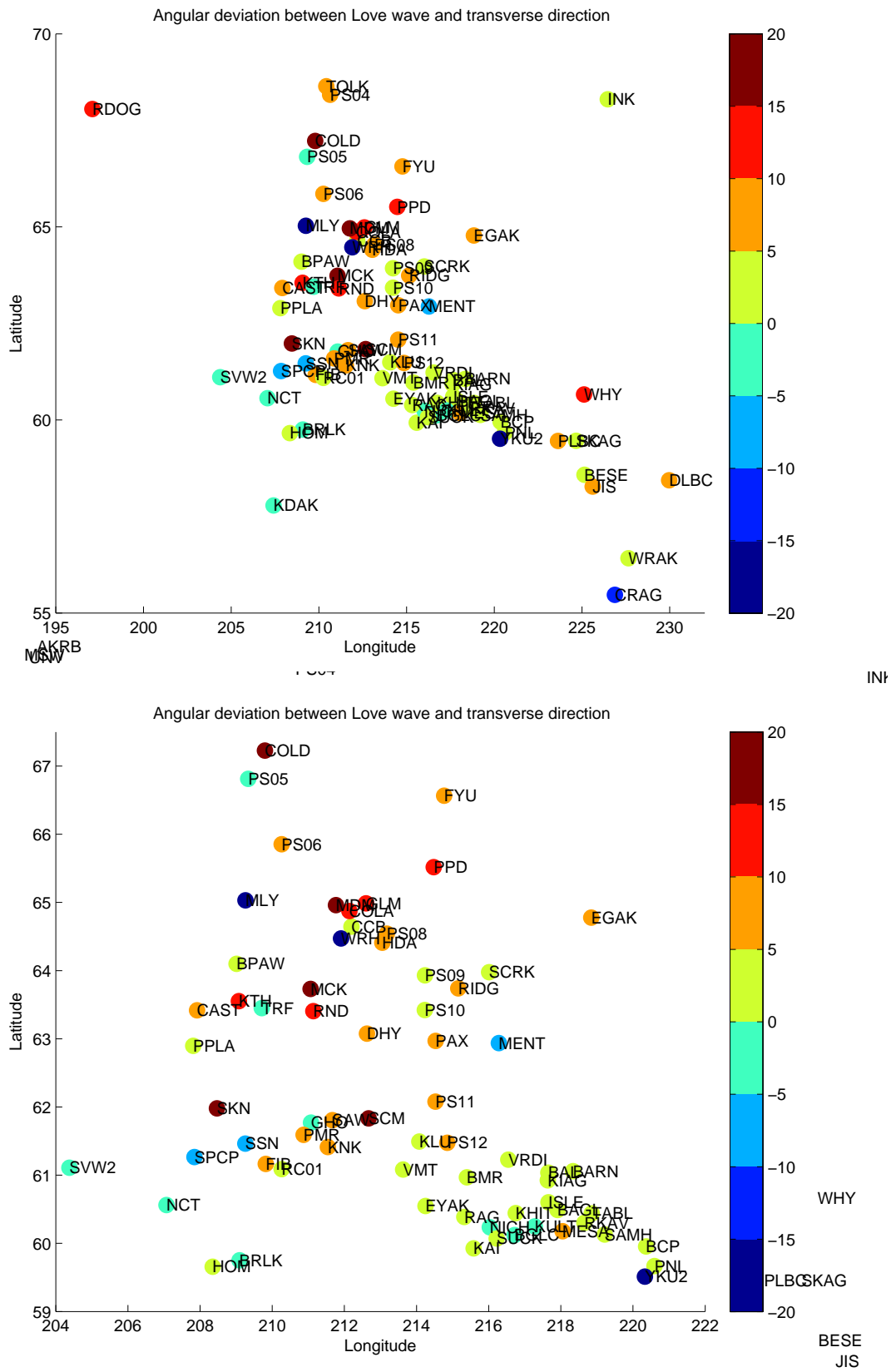


Figure 5: Angular discrepancies between the maximum horizontal displacement from Sumatra (Love wave) and the great-circle transverse component direction. No corrections have been applied. See also Table 7 and Section 4. Bottom is a zoom-in of the top view.

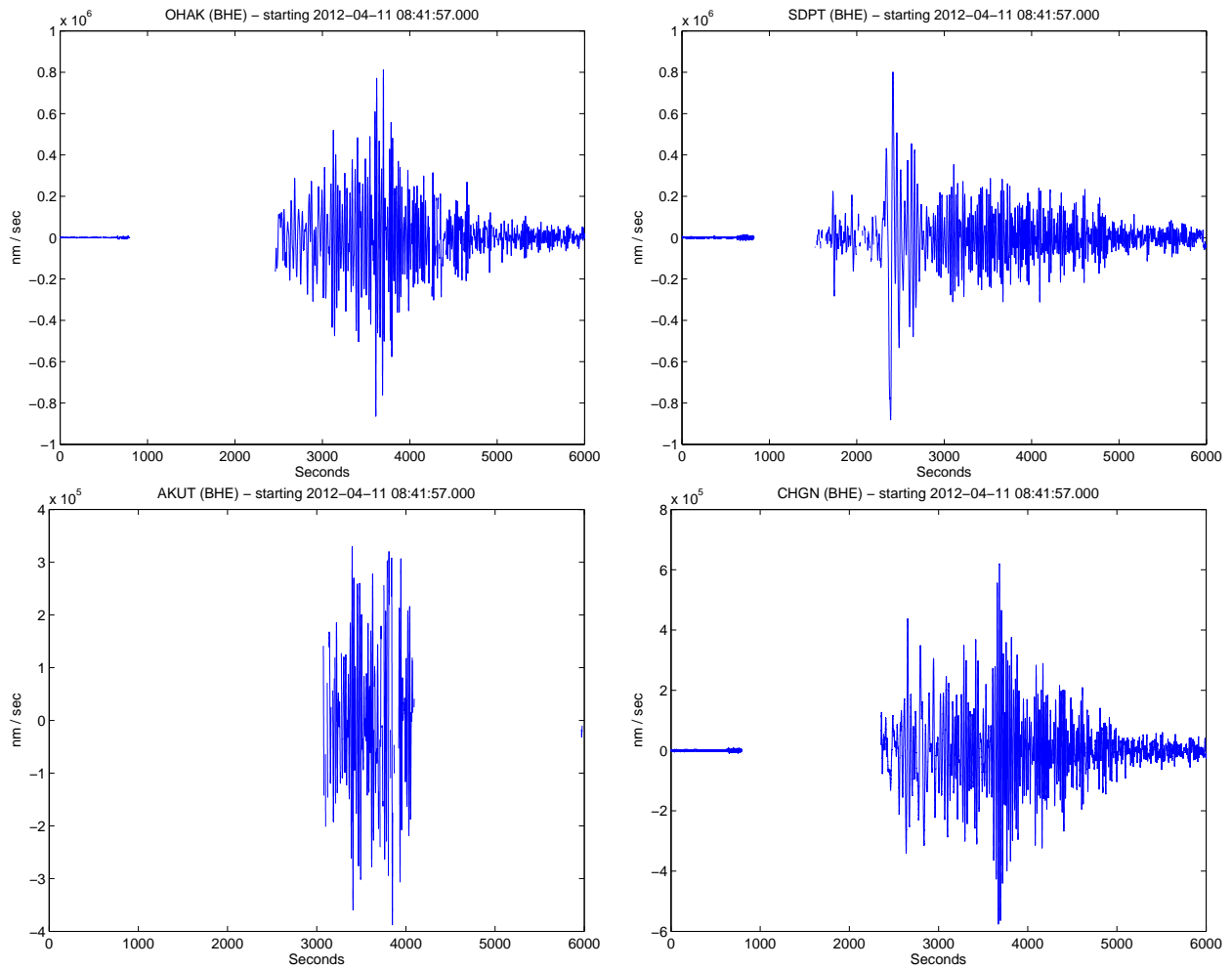


Figure 6: Examples of data gaps, shown at four AT stations (OHAK, SDPT, AKUT, CHGN). The gaps are present on all three components. Note that these gaps are different in character from those in Figure 7.

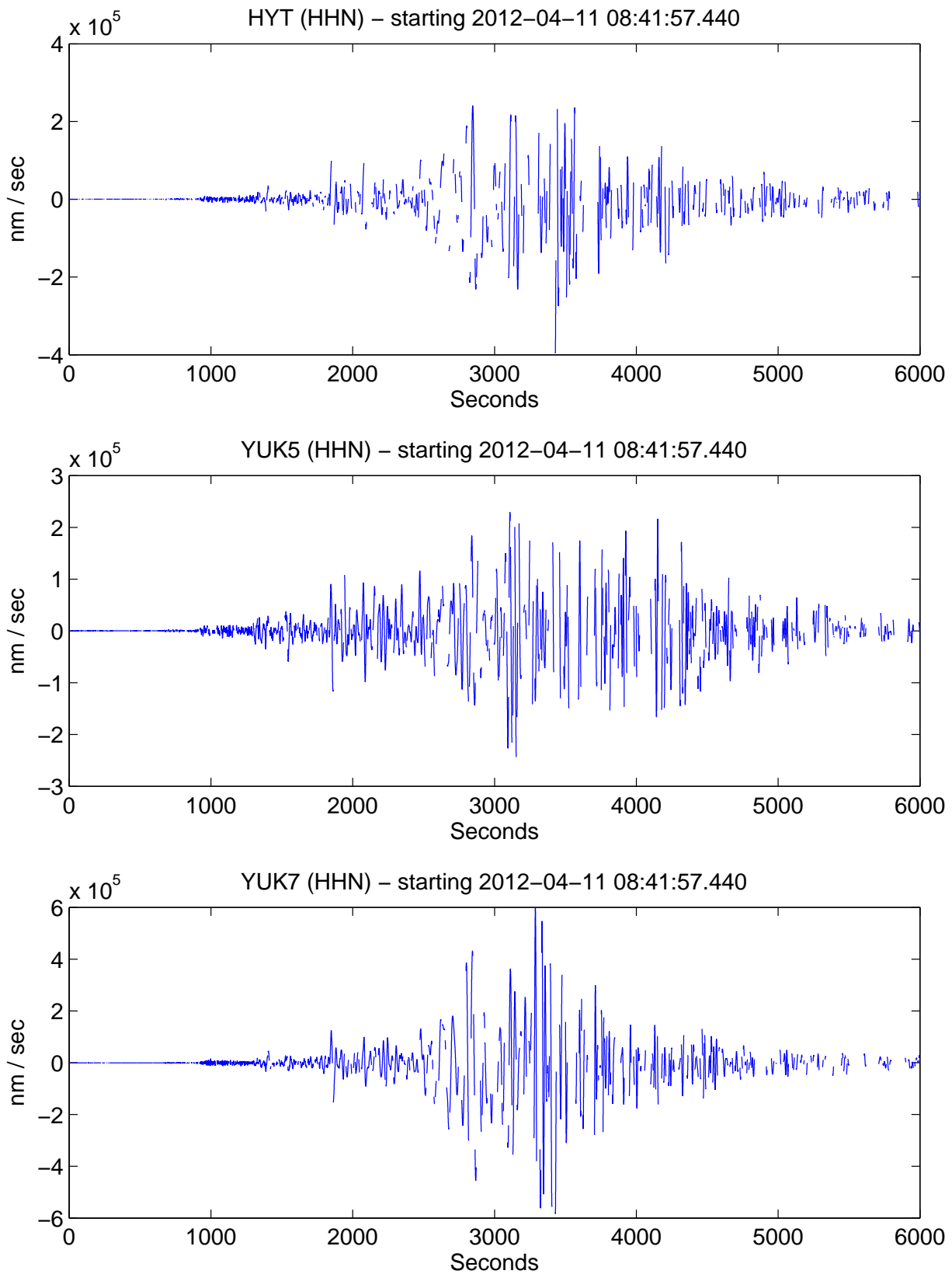


Figure 7: Examples of data gaps, shown at three CN stations (HYT, YUK5, YUK7) for the HHN channel. The gaps are present on all three components. None of these stations have data at IRIS DMC, so it is not (easily) possible to check AEC versions here with any other version. Note that these gaps are different in character from those in Figure 6.

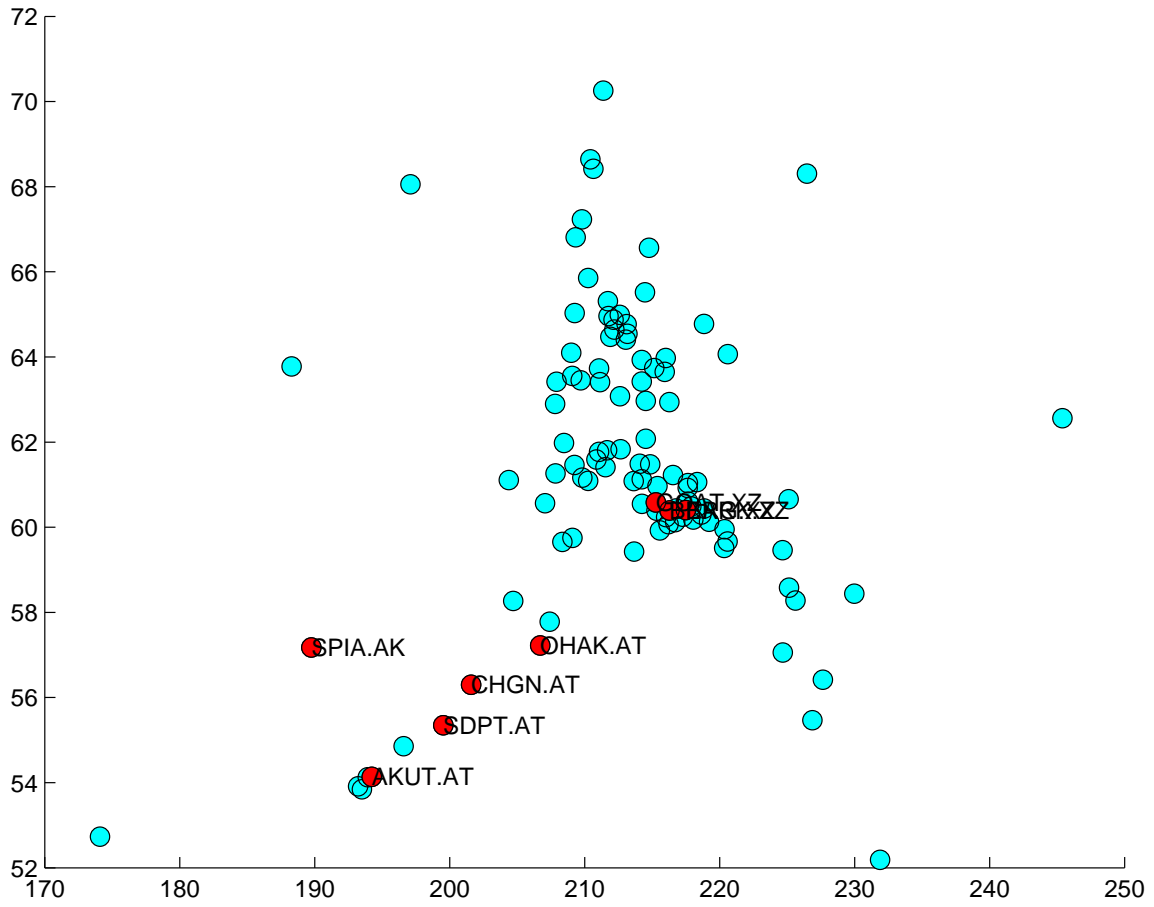


Figure 8: Map of stations with data gaps. (The AEC waveforms for CN stations, HH channel, have gaps as well.)

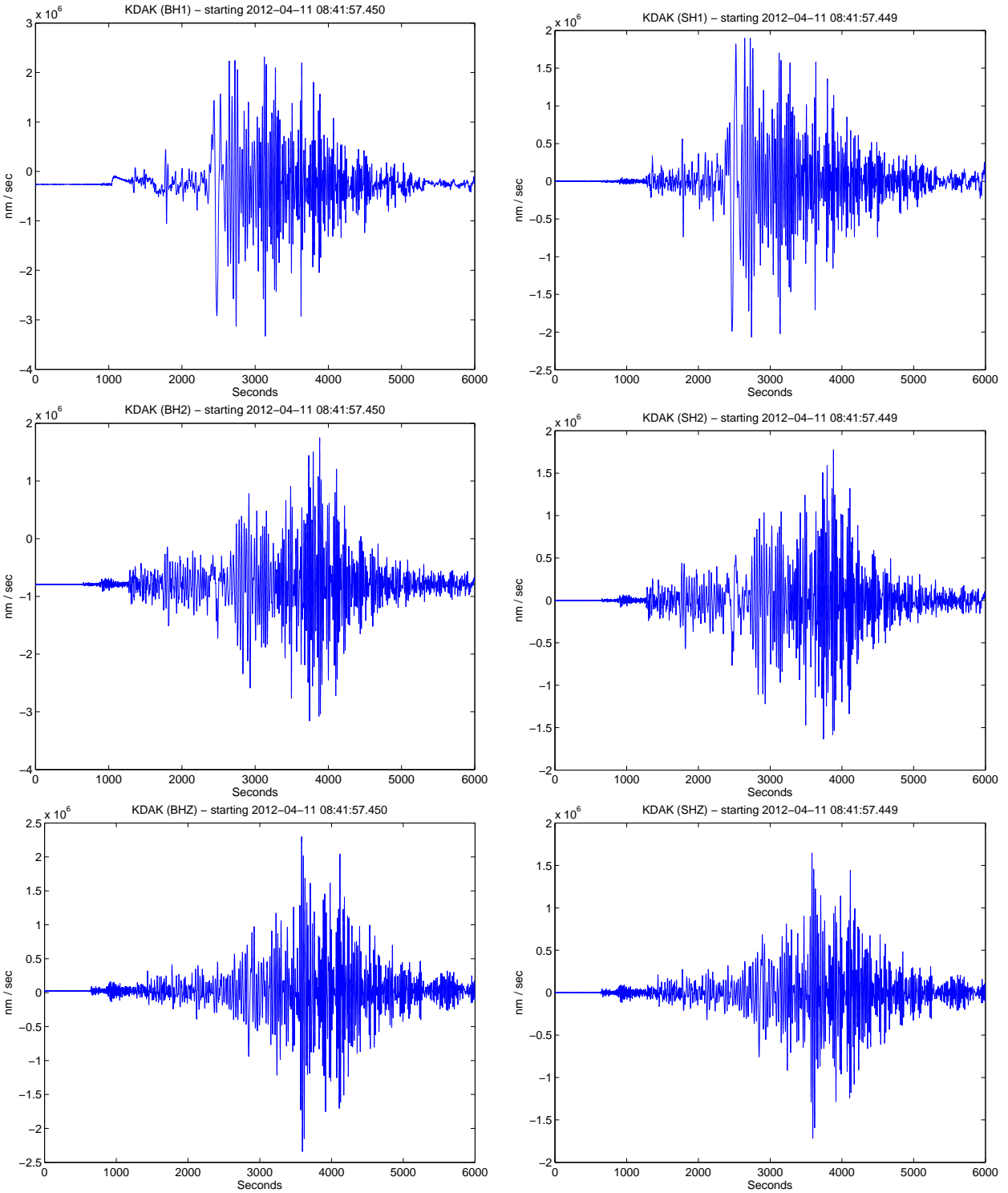


Figure 9: Raw waveforms for KDAK.II. The borehole station 1-component (BH1) has a problem early in the record that is not visible on the horizontal components of the surface station (SH1, SH2).

MENT (baz = 301.5, dist = 102.5 deg) Starting at 2012/04/11 09:16:31.120

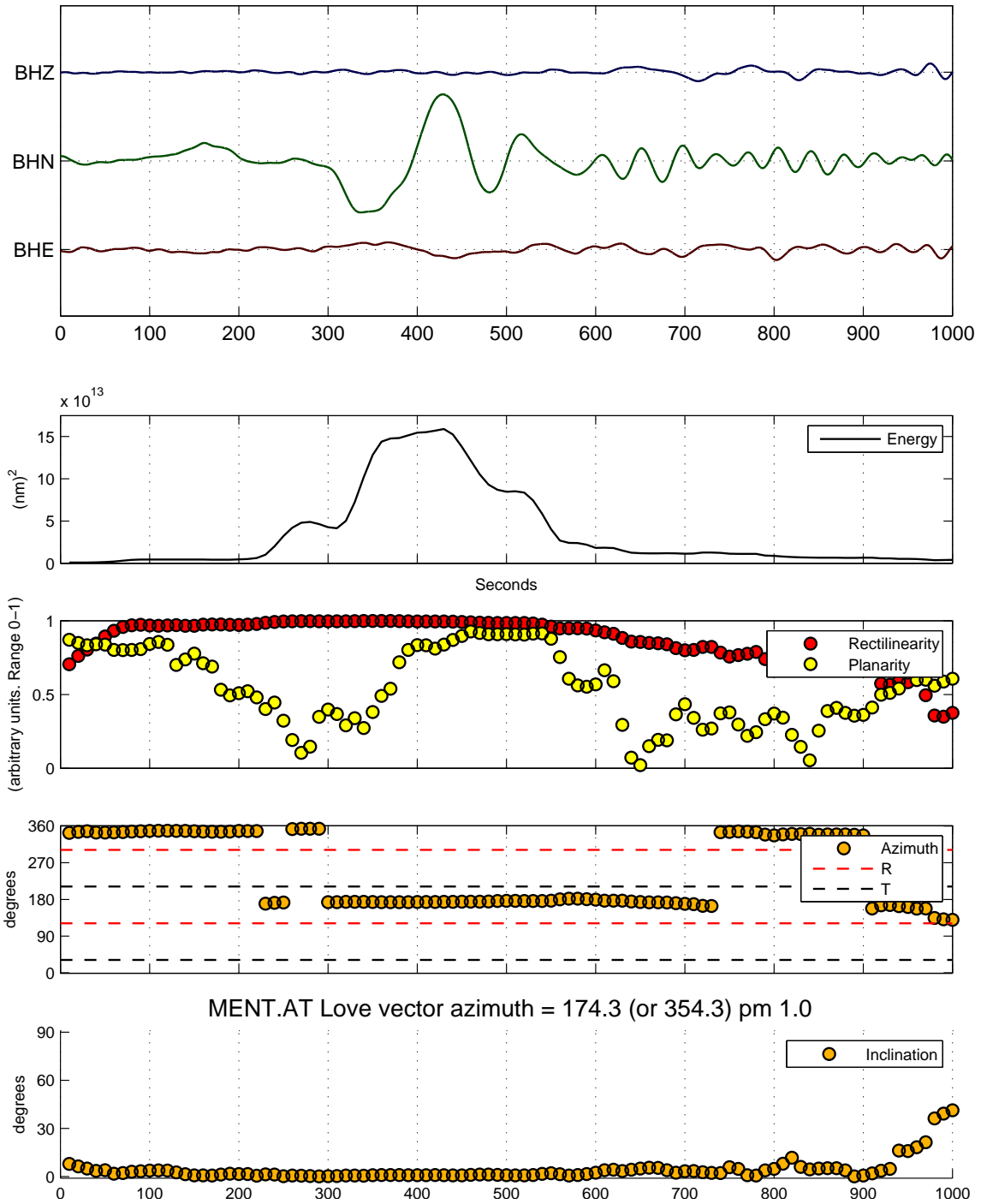


Figure 10: Example polarization analysis of the Love wave from Sumatra for one station. This station, MENT.AT, shows a deviation of -37.2° from the great-circle path (Table 7). (Figure from Version 3 report.)

BMR (baz = 300.3, dist = 103.2 deg) Starting at 2012/04/11 09:16:47.340

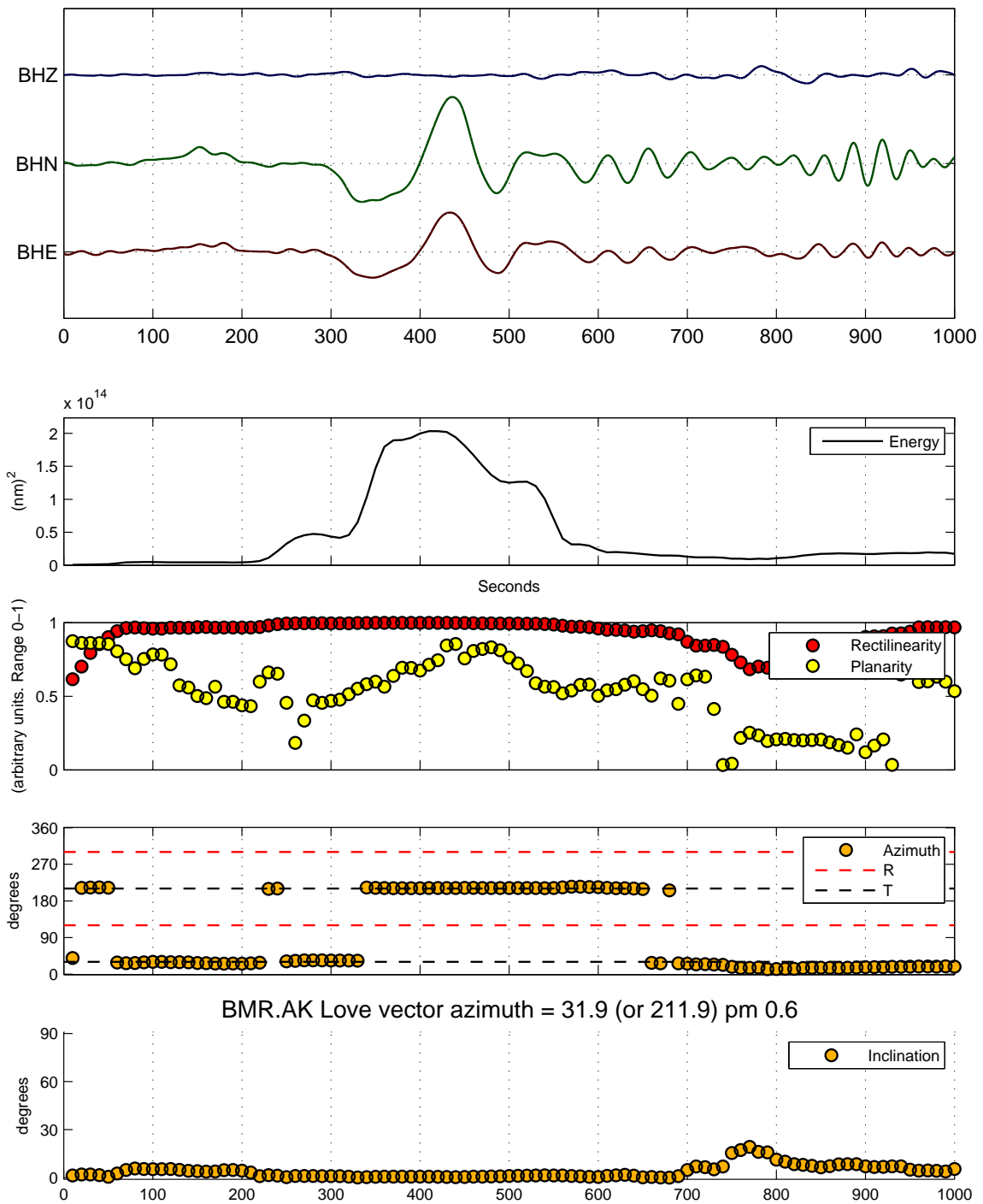


Figure 11: Example polarization analysis of the Love wave from Sumatra for one station. This station, BMR.AK, shows a deviation of 0.2° from the great-circle path (Table 7).

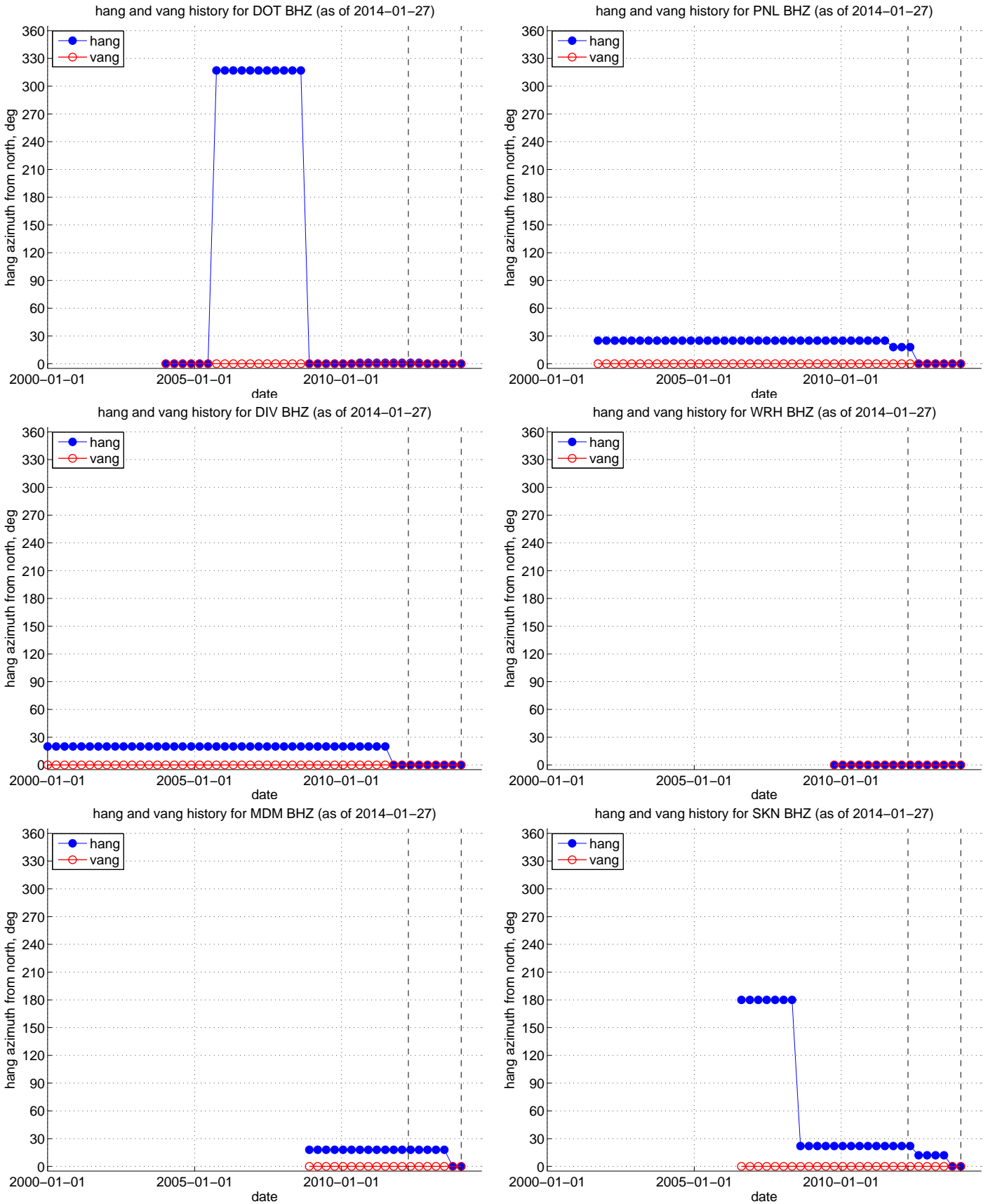


Figure 12: History of *hang* and *vang* station metadata fields at some example stations: DOT, PNL, DIV, WRH, MDM, SKN. These time histories are needed to determine whether the alignment errors identified by *Hanna and Long* (2012) are relevant at the time of 11-April-2012 (left vertical dashed line). See Section 4.

time aligned on 2012-04-11 09:21:57; YKW1 max 2.54e+07 nm at t = 893.6 s
 BHT HHT SHT [nm, --] event 201204110838A (2012-04-11, M8.6, 92.8, 2.2, z = 40.0 km)
 23 / 113 seismograms (113 stations) ordered by azimuth, norm --> none

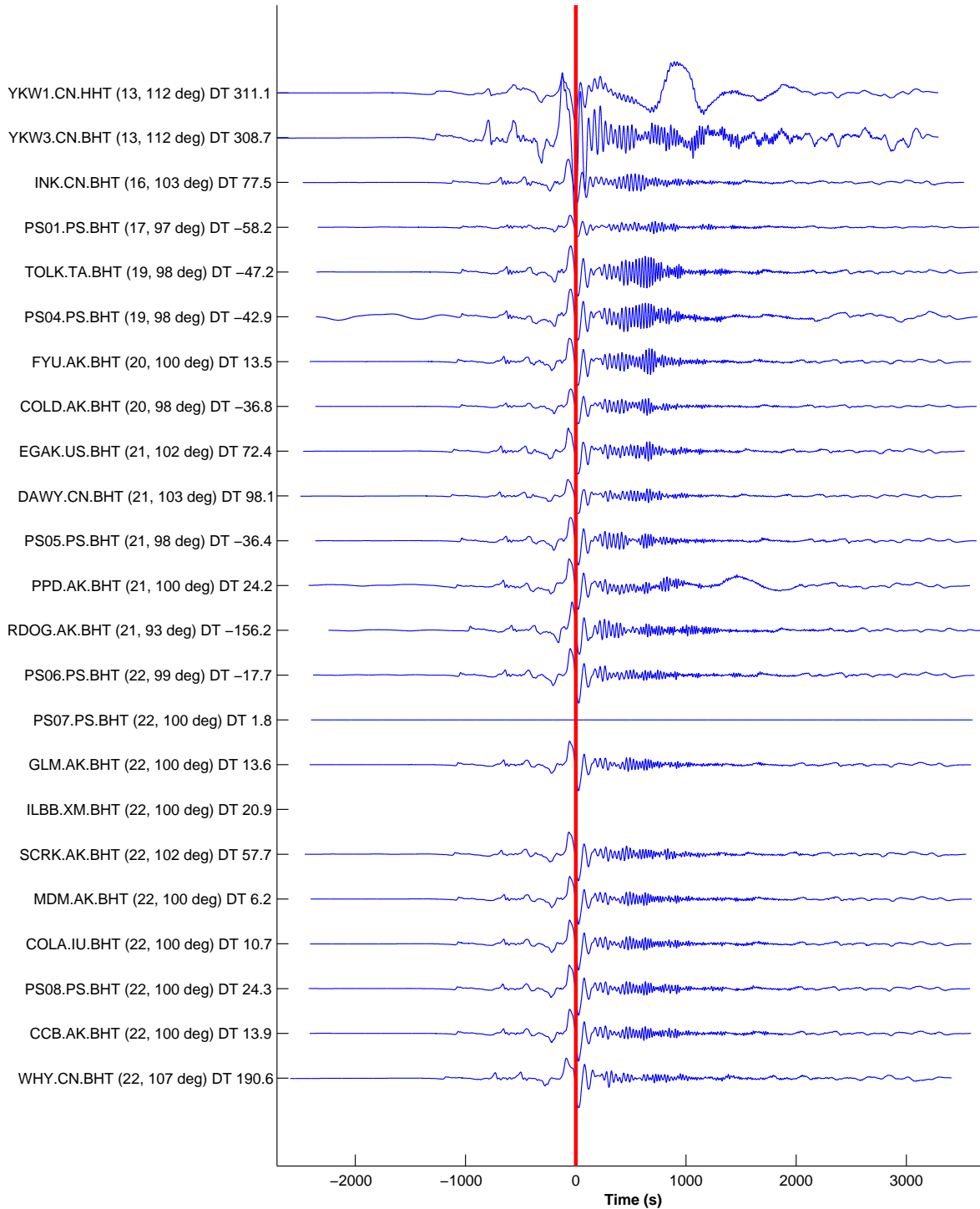


Figure 13: **PAGE 1:** Time-shifted, transverse-component Sumatra waveforms, sorted by azimuth from Sumatra. The processing involved deconvolution of instrument response over the bandpass 0.5–500 s, then detrended and integrated to displacement.

time aligned on 2012-04-11 09:21:57; HDA max $-2.22e+07$ nm at $t = 25.9$ s
 BHT HHT SHT [nm, --] event 201204110838A (2012-04-11, M8.6, 92.8, 2.2, $z = 40.0$ km)
 23 / 113 seismograms (113 stations) ordered by azimuth, norm --> none

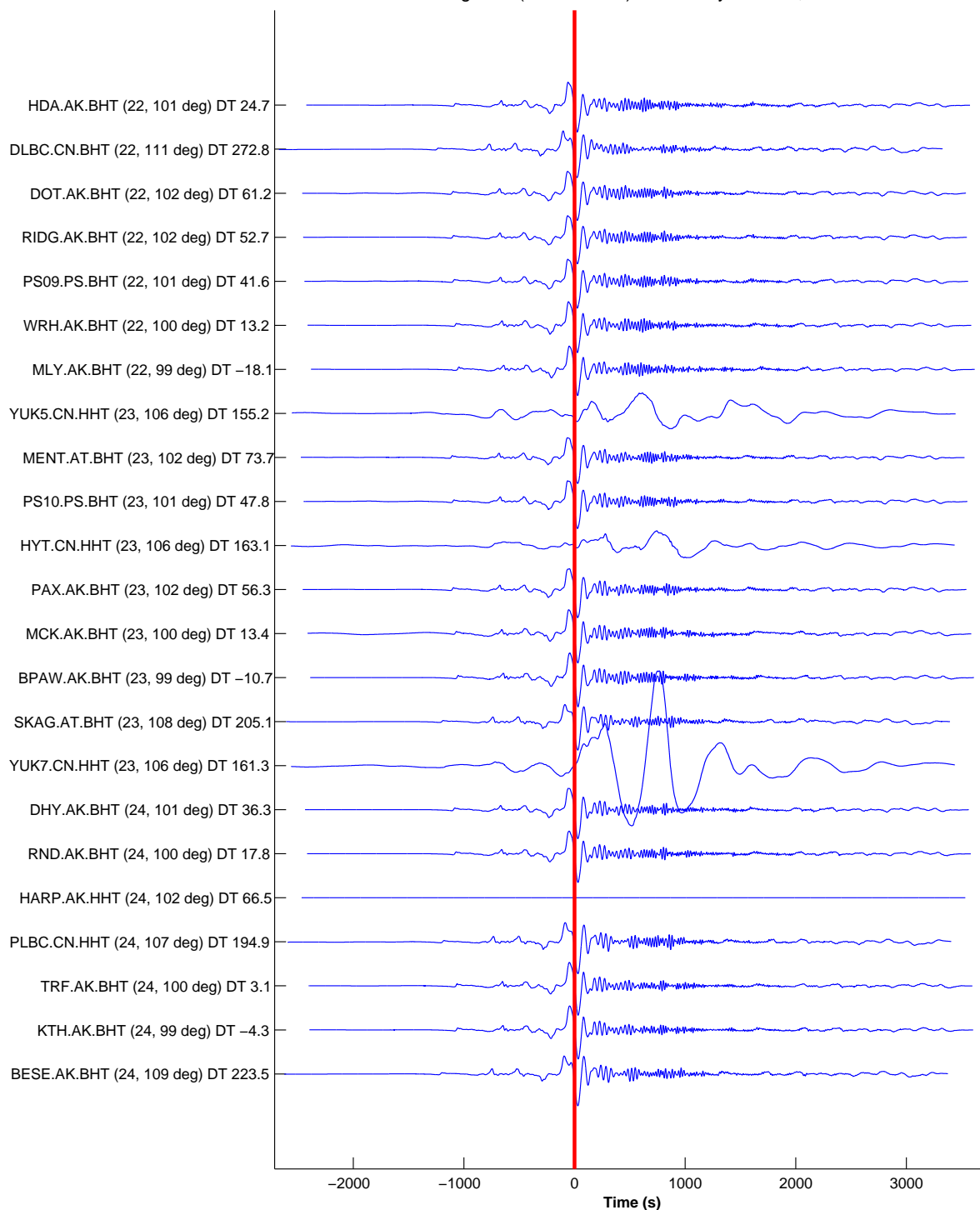


Figure 14: PAGE 2:

time aligned on 2012-04-11 09:21:57; BARN max $-2.63e+07$ nm at $t = 33.3$ s
 BHT HHT SHT [nm, --] event 201204110838A (2012-04-11, M8.6, 92.8, 2.2, $z = 40.0$ km)
 23 / 113 seismograms (113 stations) ordered by azimuth, norm --> none

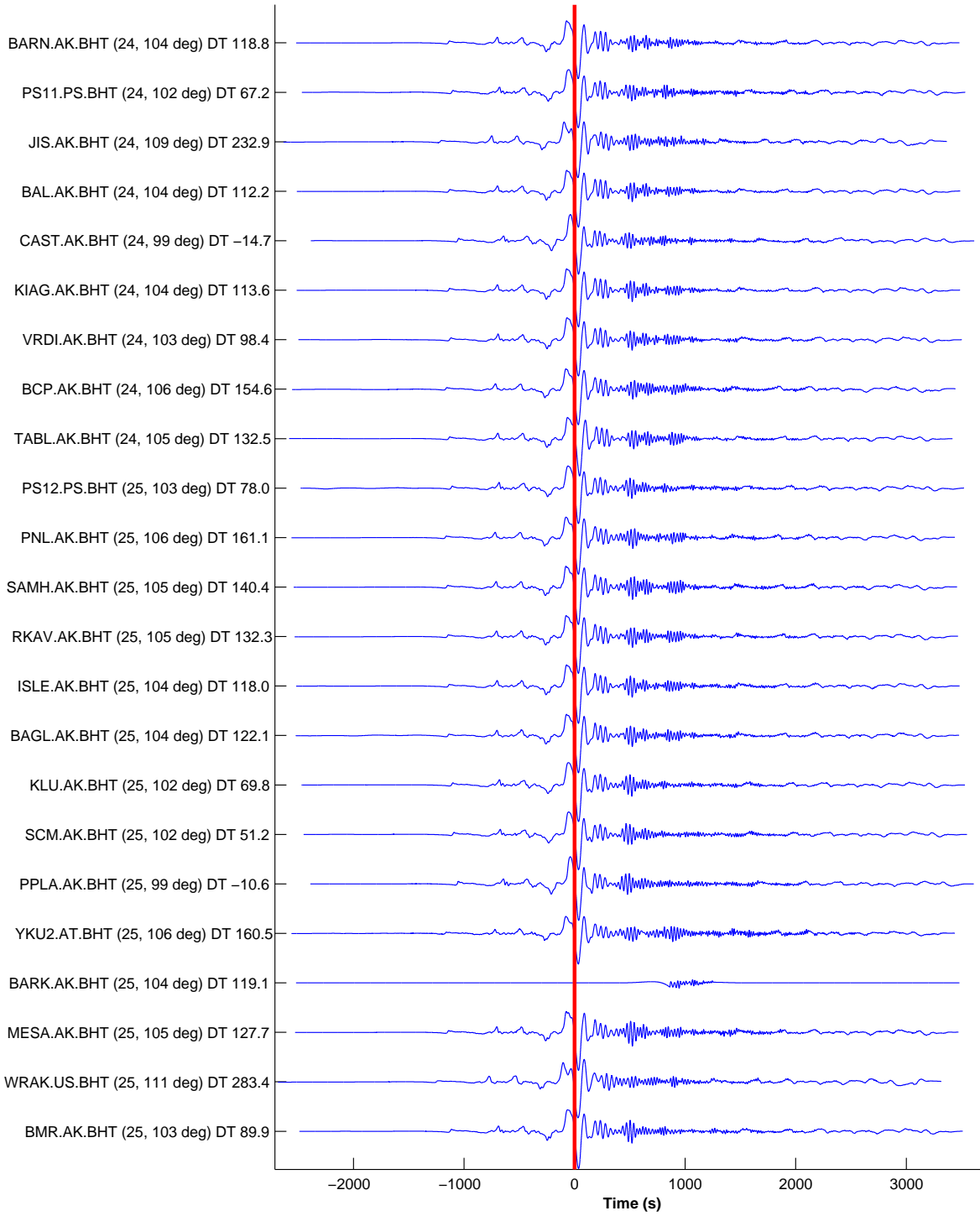


Figure 15: PAGE 3:

time aligned on 2012-04-11 09:21:57; KHIT max $-2.84e+07$ nm at $t = 36.3$ s
BHT HHT SHT [nm, --] event 201204110838A (2012-04-11, M8.6, 92.8, 2.2, $z = 40.0$ km)
23 / 113 seismograms (113 stations) ordered by azimuth, norm --> none

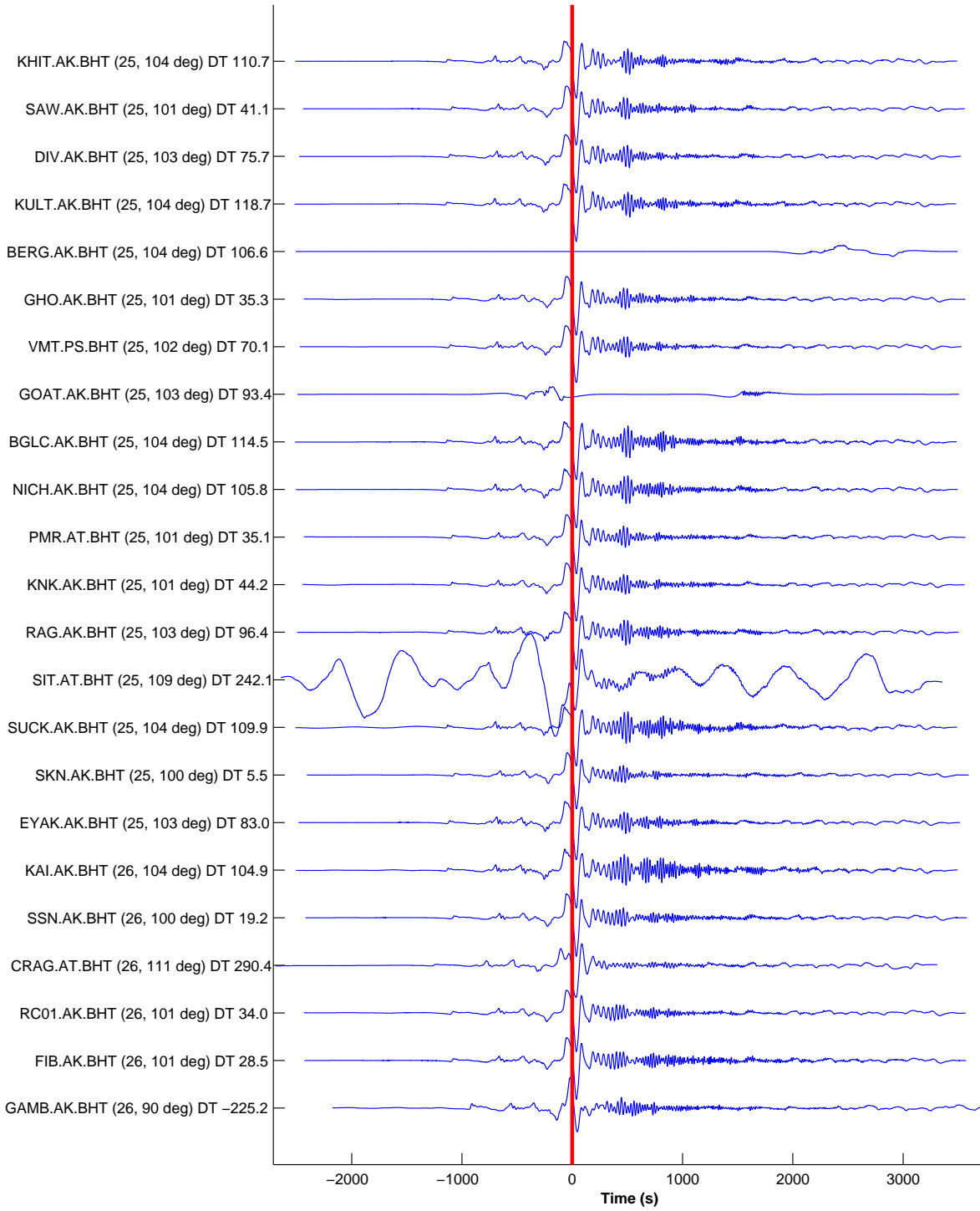


Figure 16: PAGE 4:

time aligned on 2012-04-11 09:21:57; SPCP max $-1.89e+07$ nm at $t = 39.4$ s
BHT HHT SHT [nm, --] event 201204110838A (2012-04-11, M8.6, 92.8, 2.2, z = 40.0 km)
21 / 113 seismograms (113 stations) ordered by azimuth, norm --> none

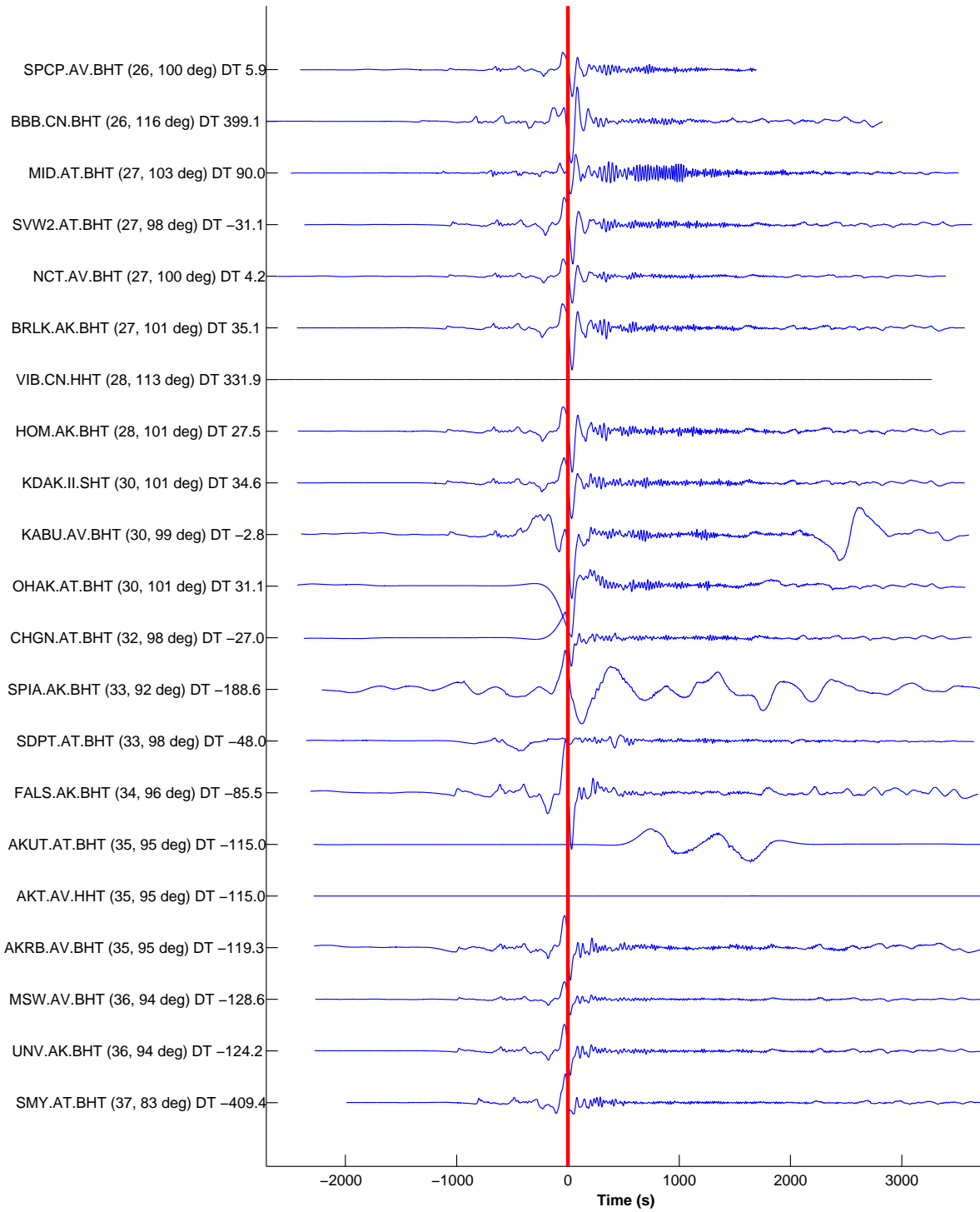


Figure 17: PAGE 5:

time aligned on 2012-04-11 09:21:57; YKW1 max -2.17×10^7 nm at $t = -5.9$ s
 BHT HHT SHT [nm, --] event 201204110838A (2012-04-11, M8.6, 92.8, 2.2, z = 40.0 km)
 23 / 113 seismograms (113 stations) ordered by azimuth, norm --> none

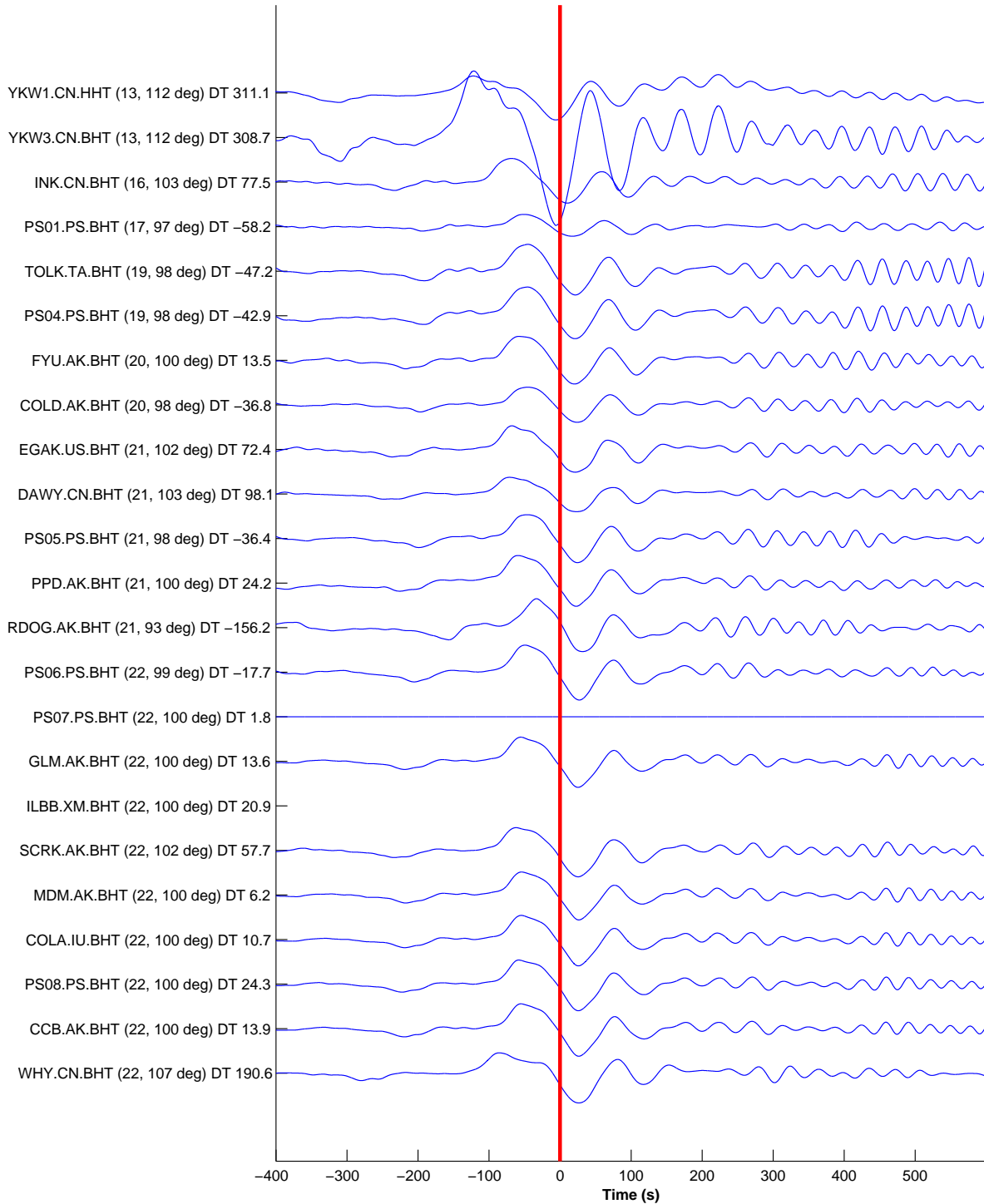


Figure 18: **PAGE 1:** Time-shifted Sumatra Love waves, sorted by azimuth from Sumatra. The processing involved deconvolution of instrument response over the bandpass 0.5–500 s, then detrended and integrated to displacement.

time aligned on 2012-04-11 09:21:57; HDA max -2.19×10^7 nm at $t = 25.9$ s
BHT HHT SHT [nm, --] event 201204110838A (2012-04-11, M8.6, 92.8, 2.2, $z = 40.0$ km)
23 / 113 seismograms (113 stations) ordered by azimuth, norm --> none

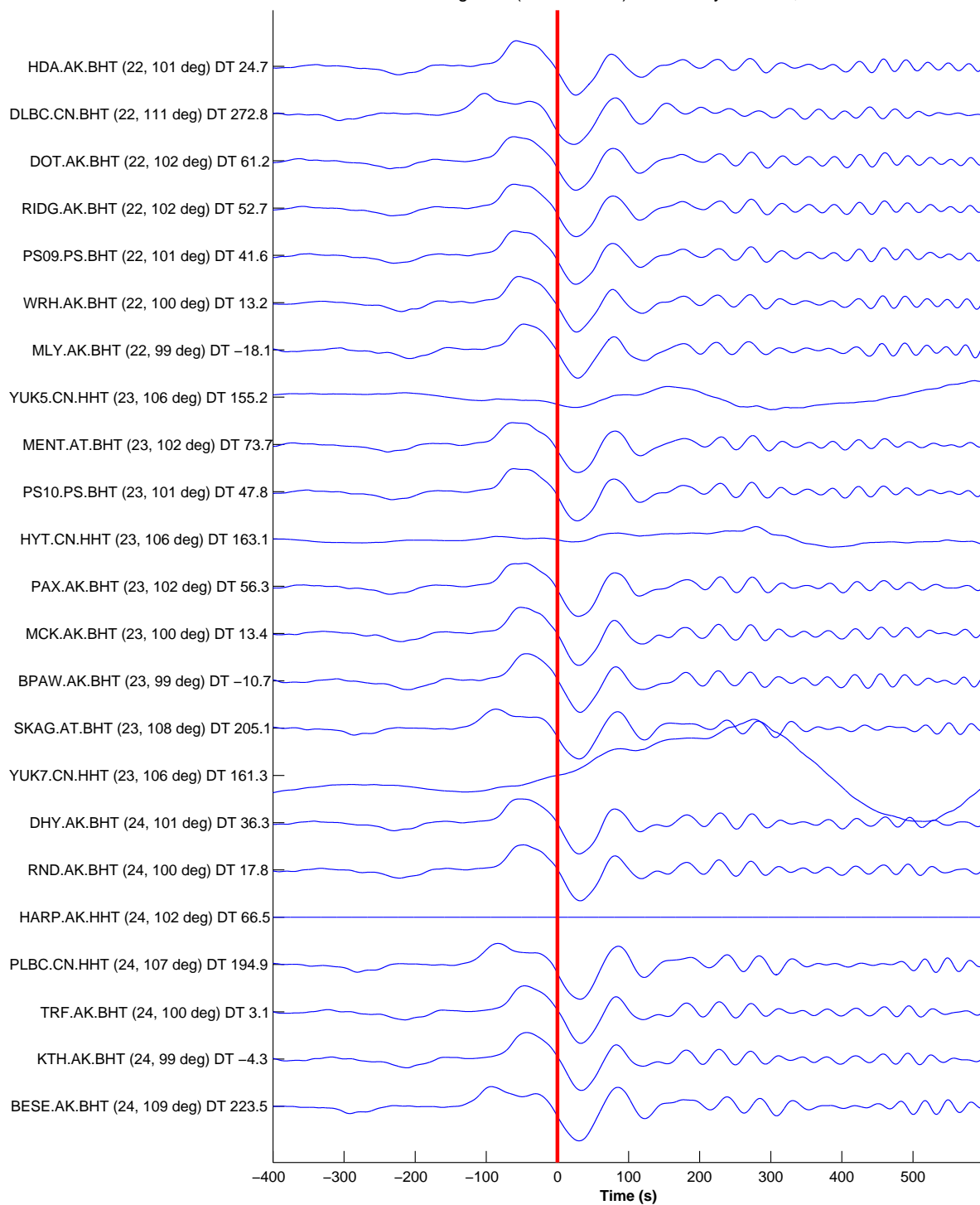


Figure 19: PAGE 2:

time aligned on 2012-04-11 09:21:57; BARN max $-2.62e+07$ nm at $t = 33.3$ s
BHT HHT SHT [nm, --] event 201204110838A (2012-04-11, M8.6, 92.8, 2.2, $z = 40.0$ km)
23 / 113 seismograms (113 stations) ordered by azimuth, norm --> none

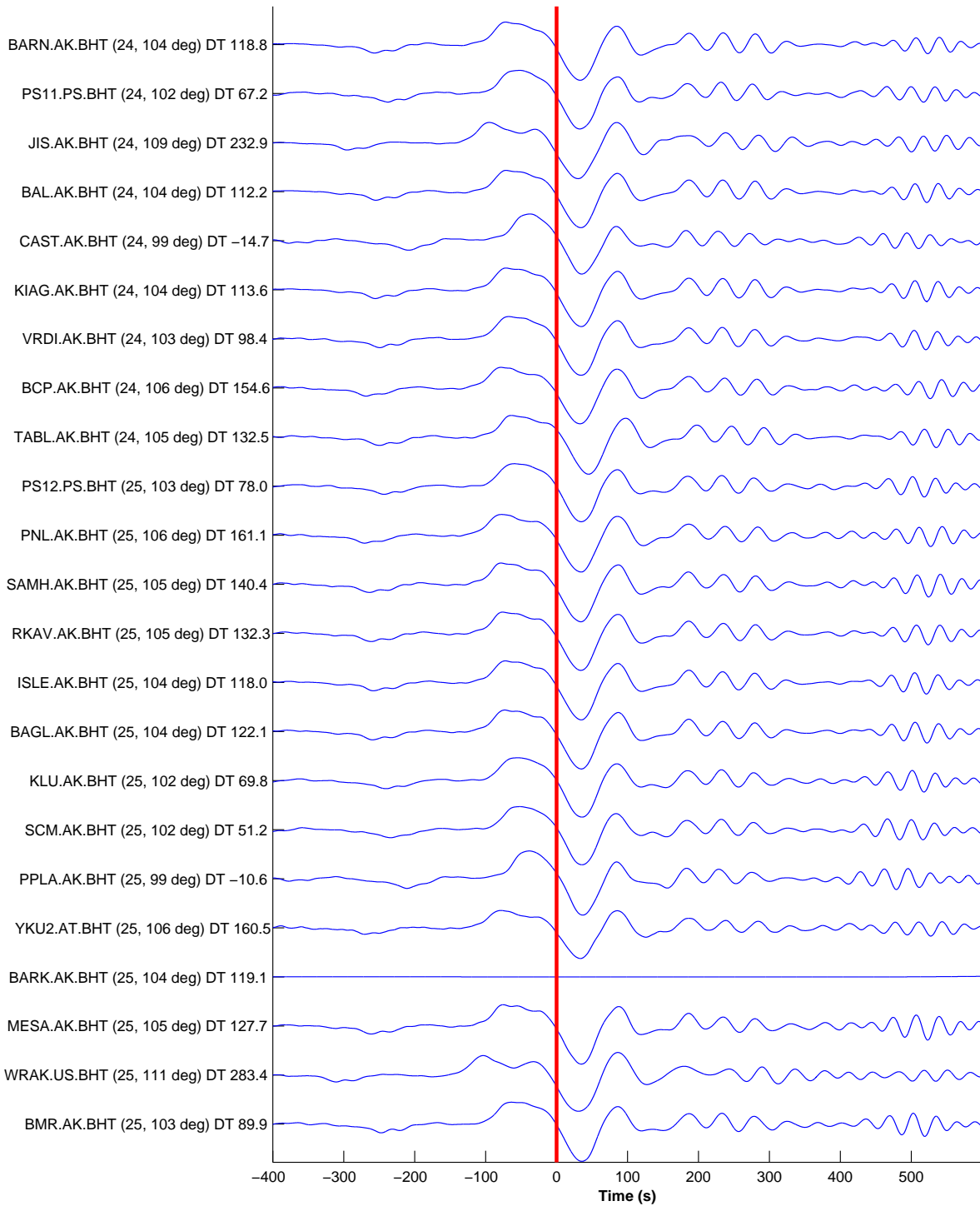


Figure 20: PAGE 3:

time aligned on 2012-04-11 09:21:57; KHIT max $-2.82e+07$ nm at $t = 36.3$ s
 BHT HHT SHT [nm, --] event 201204110838A (2012-04-11, M8.6, 92.8, 2.2, z = 40.0 km)
 23 / 113 seismograms (113 stations) ordered by azimuth, norm --> none

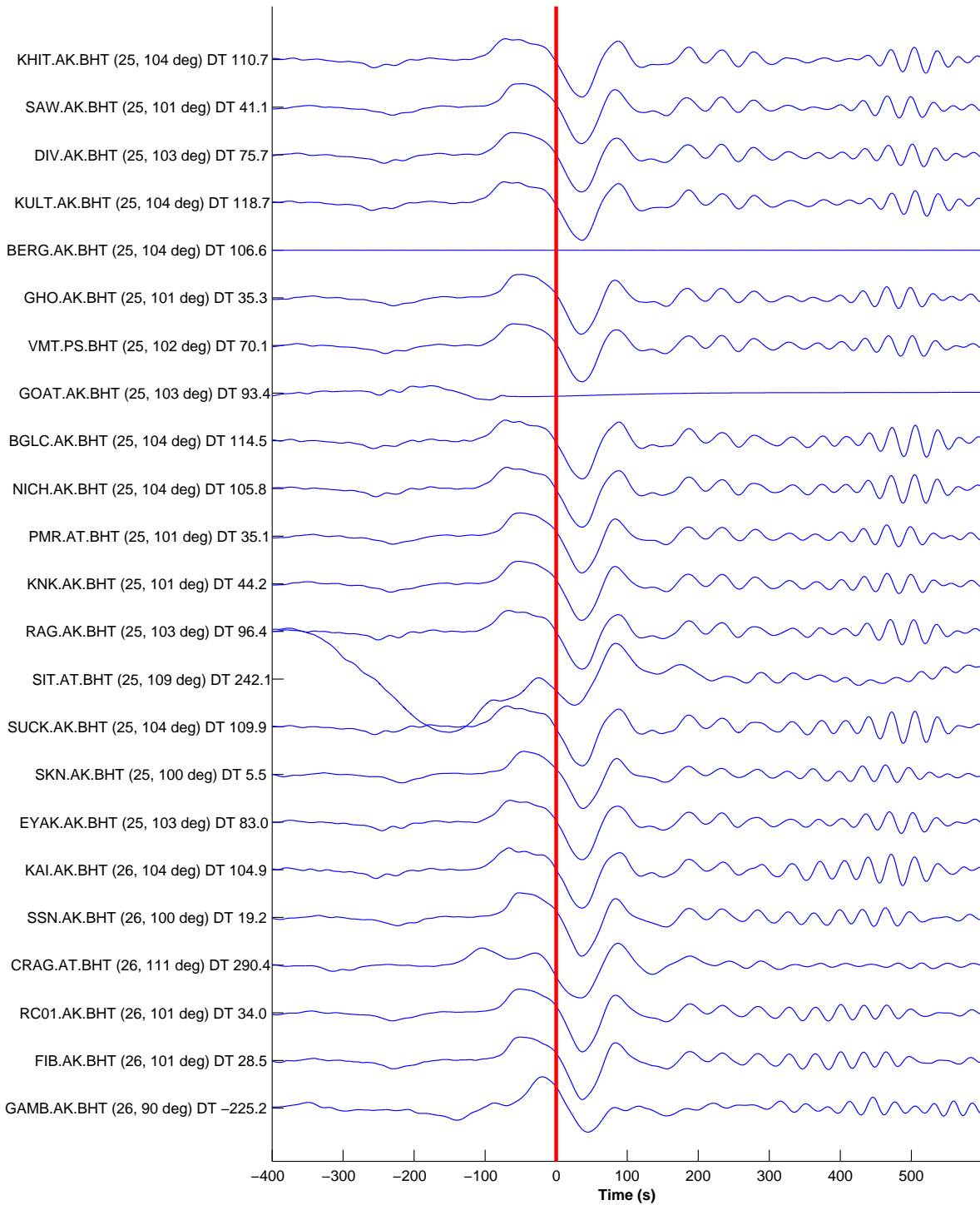


Figure 21: PAGE 4:

time aligned on 2012-04-11 09:21:57; SPCP max $-1.88e+07$ nm at $t = 39.4$ s
BHT HHT SHT [nm, --] event 201204110838A (2012-04-11, M8.6, 92.8, 2.2, $z = 40.0$ km)
21 / 113 seismograms (113 stations) ordered by azimuth, norm --> none

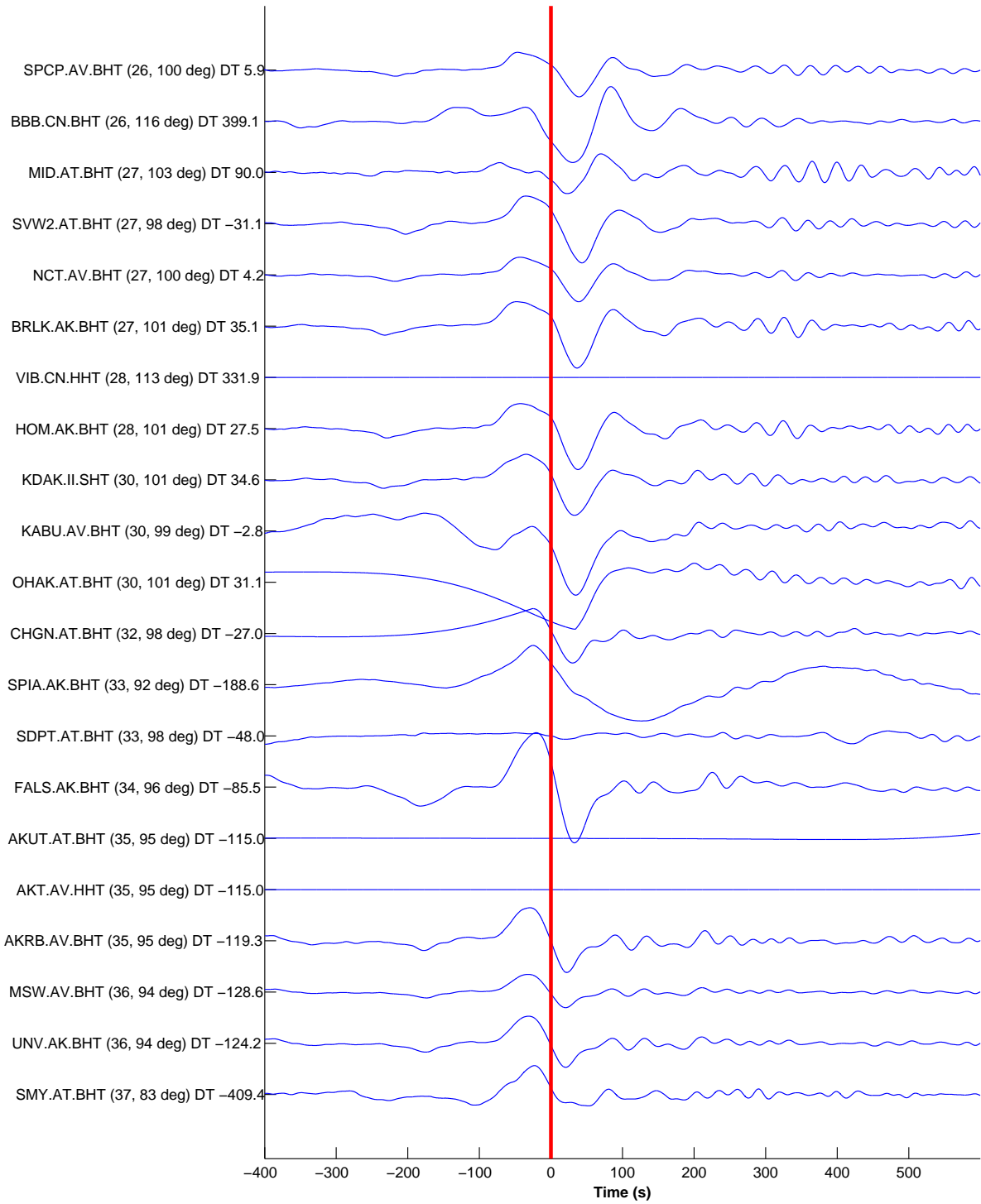


Figure 22: PAGE 5: